Published in final edited form as:
Neuropharmacology. 2010 February ; 58(2): 501. doi:10.1016/j.neuropharm.2009.08.022.

SDF-1α/CXCL12 enhances GABA and glutamate synaptic activity at serotonin neurons in the rat dorsal raphe nucleus

Silke Heinisch and **Lynn G. Kirby**
Department of Anatomy and Cell Biology & Center for Substance Abuse Research, Temple University School of Medicine, Philadelphia, PA 19140, USA.

Summary

The serotonin (5-hydroxytryptamine; 5-HT) system has a well-characterized role in depression. Recent reports describe comorbidities of mood-immune disorders, suggesting an immunological component may contribute to the pathogenesis of depression as well. Chemokines, immune proteins which mediate leukocyte trafficking, and their receptors are widely distributed in the brain, mediate neuronal patterning, and modulate various neuropathologies. The purpose of this study was to investigate the neuroanatomical relationship and functional impact of the chemokine stromal cell-derived factor-1α/CXCL12 and its receptor, CXCR4, on the serotonin dorsal raphe nucleus (DRN) system in the rat using anatomical and electrophysiological techniques. Immunohistochemical analysis indicates that over 70% of 5-HT neurons colocalize with CXCL12 and CXCR4. At a subcellular level, CXCL12 localizes throughout the cytoplasm whereas CXCR4 concentrates to the outer membrane and processes of 5-HT neurons. CXCL12 and CXCR4 also colocalize on individual DRN cells. Furthermore, electrophysiological studies demonstrate CXCL12 depolarization of 5-HT neurons indirectly via glutamate synaptic inputs. CXCL12 also enhances the frequency of spontaneous inhibitory and excitatory postsynaptic currents (sIPSC and sEPSC). CXCL12 concentration-dependently increases evoked IPSC amplitude and decreases evoked IPSC paired-pulse ratio selectively in 5-HT neurons, effects blocked by the CXCR4 antagonist AMD3100. These data indicate presynaptic enhancement of GABA and glutamate release at 5-HT DRN neurons by CXCL12. Immunohistochemical analysis further shows CXCR4 localization to DRN GABA neurons, providing an anatomical basis for CXCL12 effects on GABA release. Thus, CXCL12 indirectly modulates 5-HT neurotransmission via GABA and glutamate synaptic afferents. Future therapies targeting CXCL12 and other chemokines may treat serotonin related mood disorders, particularly depression experienced by immune-compromised individuals.

Keywords

chemokine; 5-HT; GABA; glutamate; electrophysiology; immunohistochemistry; dorsal raphe nucleus

Correspondence: Lynn G. Kirby Dept. of Anatomy and Cell Biology OMS 618 Temple University School of Medicine 3400 N. Broad St. Philadelphia, PA 19140 Phone: (215) 707-8556 Fax: (215) 707-9468 lkirby@temple.edu.

Introduction

Depression is a complex psychiatric disorder with multiple etiologies. Dysfunction of the serotonin neurotransmitter system is implicated in depression and anxiety, and clinical studies indicate that patients with chronic immunological disorders frequently experience depression (Dickens et al., 2003; Siegert and Abernethy, 2005; Evans et al., 2005; Kim et al., 2007). These patients often exhibit elevated proinflammatory cytokines, including interleukin-1, interleukin-6, and tumor necrosis factor-α, which can deplete tryptophan, the rate-limiting enzyme in serotonin biosynthesis (Dantzer and Kelley, 2007). In animal models, injection of cytokines elicits "sickness behavior" characterized by depression, anorexia, and fatigue (Reichenberg et al., 2001; Dantzer and Kelley, 2007). This has led to a "cytokine hypothesis of depression," in which cytokine hypersecretion is implicated in the pathophysiology of depression (Schiepers et al., 2005).

Chemokines (*chemo*tactic cyto*kines*) are a class of small (7-11 kD), secreted cytokines which mediate leukocyte mobilization to sites of inflammation in the periphery (Sozzani et al., 1996; Murdoch and Finn, 2000). These immune molecules and their G-protein coupled receptors have also been detected throughout the brain, an immunologically specialized tissue (Bajetto et al., 2001; Schiepers et al., 2005). In particular, CXCL12 and its receptor CXCR4 are well characterized on neurons and glia in the hippocampus, cerebral cortex, substantia nigra, striatum, hypothalamus, and globus pallidus (Bajetto et al., 1999; Banisadr et al., 2000; Banisadr et al., 2002; Banisadr et al., 2003). CXCL12 and CXCR4 are also critical for neurogenesis and neuronal migration/patterning during development (Rezaie et al., 2002; Tran et al., 2007; Stumm and Hollt, 2007). In fact, CXCR4 -/- rodents have been shown to exhibit extensive cerebellar malformations and fail to survive (Tran and Miller, 2005).

The presence and role of chemokines and chemokine receptors in the brain is actively under investigation since these immune proteins are reported to be a new class of neuromodulators (Adler et al., 2005; Adler and Rogers, 2005; Callewaere et al., 2007; Guyon and Nahon, 2007). Among the chemokines, CXCL12 has been shown to be constitutively expressed in cholinergic, dopaminergic, and vasopressinergic neurons (Banisadr et al., 2003). CXCR4 is also constitutively expressed in cholinergic and dopaminergic neurons (Banisadr et al., 2002). Electrophysiological studies of cerebellar Purkinje cells as well as hippocampal and hypothalamic neurons indicate that CXCL12 directly impacts neuronal membrane properties and indirectly impacts these cells via modulation of synaptic activity (Meucci et al., 1998; Limatola et al., 2000; Ragozzino et al., 2002; Guyon et al., 2005a; Guyon et al., 2005b; Skrzydelski et al., 2007).

The midbrain raphe nuclei (RN), comprised of the DRN and median raphe nucleus (MRN), contains the largest population of serotonergic neurons in the brain (Jacobs and Azmitia, 1992), and CXCL12 has been shown to be expressed in the DRN (Banisadr et al., 2003). However, the localization of CXCL12 and CXCR4 to 5-HT neurons, and the functional impact of CXCL12 on 5-HT neurotransmission have not been examined. The ability of chemokines to modulate the serotonin system may affect the pathophysiology and treatment of depressive disorders associated with immunological dysfunction. The purpose of this study was to examine the neuroanatomical localization of CXCL12 and CXCR4 in relation to 5-HT neurons and to determine the electrophysiological actions of CXCL12 on 5-HT neurons using immunohistochemistry and whole-cell patch-clamp recordings in an *in vitro* slice preparation of the rat DRN.

Methods

Animals

Male Sprague-Dawley rats (Taconic Farms, Germantown, NY), 10 weeks of age (for immunohistochemistry) and 4-5 weeks of age (for electrophysiology) were housed 2 per cage on a 12-h light schedule (lights on at 07:00 AM) in a temperature-controlled (20°C) colony room. Rats were given access to standard rat chow and water *ad libitum*. Animal protocols were approved by the Institutional Animal Care and Use Committee and were conducted in accordance to the NIH Guide for the Care and Use of Laboratory Animals.

Antibodies

Details regarding the primary and secondary antibodies used in our immunohistochemistry experiments are provided in Table 1.

A polyclonal goat antibody prepared against a synthetic peptide corresponding to 19 amino acids in the C-terminus of CXCL12 of human origin was obtained from Santa Cruz Biotechnology, Inc. (Santa Cruz, CA). Western blot analysis with the polyclonal goat antibody from Santa Cruz recognized a single band (Miller et al., 2005; Tan et al., 2007) corresponding to the 10 kD molecular weight of CXCL12 (De Paepe et al., 2004; Kryczek et al., 2005). Preabsorption of the CXCL12 antibody with a tenfold excess of the immunogenic peptide (sc-6193P, Santa Cruz Biotechnology, Inc.) eliminated any specific staining (see Fig. 1H), confirming preabsorption controls for this antibody (Banisadr et al., 2003; Miller et al., 2005). Furthermore, immunolabeling with this antibody produced a localization profile corresponding with *in situ* hybridization for CXCL12 mRNA in neurons in the cerebral cortex, hippocampal formation, and amygdala (Stumm et al., 2002; Lu et al., 2002; Stumm and Hollt, 2007). The immunolocalization of CXCL12 in brain sections was consistent with previous studies in the cerebral cortex, hippocampus, substantia innominata, globus pallidus, paraventricular and supraoptic hypothalamic nuclei, lateral hypothalamus, substantia nigra, and oculomotor nuclei using the Santa Cruz CXCL12 antibody (Banisadr et al., 2003; Miller et al., 2005; Callewaere et al., 2006) as well as other CXCL12 antibodies (Stumm et al., 2002).

To detect CXCR4-immunoreactivity in the rat brain, we used a polyclonal goat antibody prepared from a 20 amino acid peptide to the C-terminus of CXCR4 receptor of human origin obtained from Santa Cruz Biotechnology, Inc. In western blot analysis, the antibody revealed a 45 kD band in both cultured neurons and rat brain samples, corresponding to the expected molecular mass for CXCR4 (Pujol et al., 2005). Preincubation of the polyclonal goat CXCR4 antibody overnight with a tenfold excess of the immunogenic peptide (sc-6190P, Santa Cruz Biotechnology, Inc.), eliminated specific staining (see Fig. 1H), confirming preabsorption controls for this antibody (Banisadr et al., 2002). Furthermore, immunolabeling with this antibody produced a localization profile matching *in situ* hybridization for CXCR4 mRNA in neurons in the ventricular ependyma, olfactory bulb, cerebral cortex, hippocampus, amygdala, caudate putamen, and cerebellum (Stumm et al., 2002; Lu et al., 2002; Stumm et al., 2007). The immunolocalization of CXCR4 in brain sections was consistent with previous studies in the cerebral cortex, caudate putamen, globus pallidus, substantia innominata, supraoptic and paraventricular hypothalamic nuclei, ventromedial thalamic nucleus, substantia nigra, and hippocampus using the Santa Cruz CXCR4 antibody (Banisadr et al., 2002; Baudouin et al., 2006) as well as other CXCR4 antibodies (Stumm et al., 2002).

Immunohistochemistry

(Antibody details in *Antibodies* section)

Rats were deeply anesthetized with pentobarbital (60 mg/kg, i.p.) and transcardially perfused with saline and 4% paraformaldehyde. Brains were extracted and cryoprotected in a 20% sucrose solution, frozen at −80°C, and sectioned coronally (30 μm) by cryostat. Midbrain sections containing the DRN and MRN were preincubated with blocking solution containing 3% normal donkey serum and 0.5% Triton X-100 in PBS for 30 min.

To analyze colocalization of CXCL12 or CXCR4 with serotonergic neurons, midbrain sections were initially coincubated with either goat anti-CXCL12 antibody (1:100; Santa Cruz Biotechnology, Inc.) or goat anti-CXCR4 antibody (1:100; Santa Cruz Biotechnology, Inc.) and with mouse anti-tryptophan hydroxylase (TPH) antibody (1:500; Sigma-Aldrich, St. Louis, MO) overnight at 4°C. Subsequently, immunohistochemical labeling was probed with an Alexa 647-conjugated donkey anti-goat secondary antibody (1:200; Molecular Probes, Eugene, OR) to detect CXCL12 or CXCR4 and an Alexa 488-conjugated donkey anti-mouse secondary antibody (1:200; Molecular Probes) to detect TPH, for 1 h at room temperature in the dark.

Chemokine and chemokine receptor colocalization in the raphe nuclei was examined by incubating brain sections with antibodies directed towards CXCL12 and CXCR4. We placed the tissue in rabbit anti-CXCL12 antibody (1:100; Torrey Pines Biolabs) and goat anti-CXCR4 antibody (1:100; Santa Cruz Biotechnology, Inc.) overnight at 4°C. Next, brain sections were placed in a cocktail of Alexa Fluor 647-conjugated donkey anti-goat secondary antibody (1:200; Molecular Probes) to detect CXCR4, and Alexa Fluor 488-conjugated donkey anti-rabbit secondary antibody (1:200; Molecular Probes) to detect CXCL12, for 1 h at room temperature in the dark.

Double staining for GAD 65/67 and CXCR4 was performed in sections (60 μm) post-fixed for 2 h in 4% paraformaldehyde. Sections were transferred to PBS and 0.1% sodium azide at 4°C until staining. Sections were subsequently incubated in PBS containing 10% donkey serum for 1 h and placed in rabbit anti-GAD 65/67 antibody (1:200; Millipore, Billerica, MA) with 3% donkey serum and PBS for 4 h. The brain sections were further incubated in 0.25% Triton-X-100 in PBS for 1 hr and then placed in goat anti-CXCR4 antibody (1:100; Santa Cruz Biotechnology, Inc.) overnight at 4°C. Immunohistochemical labeling was detected with an Alexa 488-conjugated donkey anti-rabbit antibody and Alexa 647-conjugated donkey anti-goat antibody (1:200; Molecular Probes) for 4 h in the dark. All incubations were conducted at room temperature unless otherwise noted.

For all immunohistochemical experiments, brain sections were rinsed with phosphate buffer solutions (3 × 10 min) between incubations. Sections were mounted on Superfrost Plus slides (Fisher Scientific, Pittsburgh, PA) and coverslipped with Prolong Gold Antifade Reagent (Molecular Probes) or Vectashield mounting medium with DAPI (Vector Labs, Burlingame, CA).

Fluorescence Microscopy

Fluorescent images of TPH, GAD 65/67, CXCL12, or CXCR4 were captured with a Leica DMIRE TCS SL-Conformation confocal microscope using a 40× oil immersion objective and Leica operating software (Leica Microsystems, Exton, PA). The laser power and emission filters were adjusted for the red and green fluorophors to ensure a minimal possibility of a false positive result. Fluorescent photomicrographs were produced from six stacks with four-point line averaging. The image format was 1285 by 1285 pixels, and the scan speed was 400 image-lines/s. Fluorescent images were also captured with a Nikon E800 fluorescent microscope (Nikon Instruments, Melville, NY), using a Retiga EXi Fast 1394 digital camera and QCapture Suite imaging software (Quantitative Imaging Corp., Surrey, BC, Canada).

Quantification Analysis

The Vectashield mounting medium containing DAPI, which detects nuclear DNA, was applied to midbrain sections previously incubated with antibodies to detect TPH and either CXCL12 or CXCR4, to simplify the localization and quantification of single-labeled and double-labeled cells. Individual TPH (green), CXCL12 or CXCR4 (red), and DAPI (blue) fluorescent photomicrographs were captured by digital camera and QCapture imaging (*Fluorescence Microscopy* section). All DAPI-labeled cells expressing TPH were counted in the DRN (dorsomedial (DM), lateral wing (LW), and ventromedial (VM) subdivisions) and MRN and subsequently classified as "total TPH-labeled" cells. The individual green, red, and blue images were then merged using Photoshop software. Cells (DAPI-positive, blue) expressing both TPH (green) and the chemokine or chemokine receptor of interest (red) were counted and classified as "colocalized" cells. For quantification purposes, the term "colocalized" was used to identify any cell that contained green and red labeling even if the immunolabeling was present in different cellular regions, i.e. outer membrane vs. cytoplasm. Also, it is important to note that the inclusive term "colocalization" does not rule out the expression of the chemokine proteins in terminals that are synapsing onto, and thus are associated with the cell body or process.

Furthermore, "single-labeled" TPH neurons were determined by subtracting "colocalized" from "total TPH-labeled" cells. The percent of chemokine/chemokine receptor colocalization with TPH was determined by dividing the number of "colocalized" neurons by the "total TPH-labeled" neurons. Additionally, the subcellular immunolabeling observed in this study were described as puncta, cell-filled, and outer membrane.

Slice Preparation

Rats were rapidly decapitated, and the head placed in ice cold artificial cerebrospinal fluid (ACSF) in which sucrose (248 mM) was substituted for NaCl. The brain was rapidly removed and trimmed to isolate the brainstem region. Slices 200 μm thick were cut throughout the rostro-caudal extent of the midbrain RN using a Vibratome 3000 Plus (Vibratome, St. Louis, MO) and placed in a holding vial containing ACSF with l-tryptophan (50 μM) at 35°C bubbled with 95% O_2/5% CO_2 for 1 h. Slices were then maintained in ACSF at room temperature bubbled with 95% O_2/5% CO_2. The composition of the ACSF was (in mM), NaCl 124, KCl 2.5, NaH_2PO_4 2, $CaCl_2$ 2.5, $MgSO_4$ 2, Dextrose 10 and $NaHCO_3$ 26.

Electrophysiological Recordings

Slices were transferred to a recording chamber (Warner Instruments, Hamden, CT) and continuously perfused with ACSF at 1.5-2.0 ml/min at 32-34°C maintained by an in-line solution heater (TC-324, Warner Instruments). Raphe neurons were visualized using a Nikon E600 upright microscope fitted with a 40X water-immersion objective, differential interference contrast, and infrared filter (Optical Apparatus, Ardmore, PA). The image from the microscope was enhanced using a CCD camera and displayed on a computer monitor. Whole-cell recording pipettes were fashioned on a P-97 micropipette puller (Sutter Instruments, Novato, CA) using borosilicate glass capillary tubing (1.2 mm OD, 0.69 mm ID; Warner Instruments). The resistance of the electrodes was 4-8 MΩ when filled with an intracellular solution of (in mM) Kgluconate 70, KCl 70, NaCl 2, EGTA 4, HEPES 10, MgATP 4, Na_2GTP 0.3, 0.1% Biocytin, pH 7.3 for recordings of GABA synaptic activity. The intracellular solution to record membrane potential or glutamate synaptic activity was (in mM) Kgluconate 130, NaCl 5, $MgCl_2$ 1, EGTA 0.02, HEPES 10, sodium phosphocreatinine 10, MgATP 2, Na_2GTP 0.5, 0.1% Biocytin, with a final pH of 7.3. Recordings were conducted in cells located in the ventromedial subdivision of rostral-mid DRN slices corresponding to −7.56 to −8.28 mm from bregma in Paxinos and Watson (2005), an area containing dense clusters of 5-HT neurons. A visualized cell was approached with the electrode to establish a gigaohm seal, and the cell membrane was subsequently ruptured to obtain a whole-cell recording configuration using a HEKA patch

clamp EPC-10 amplifier (HEKA Elecktronik, Pfalz, Germany). Series resistance was monitored throughout the experiment. If the series resistance was unstable or exceeded four times the electrode resistance during the experiment then the cell was discarded. When the whole-cell configuration was obtained in a stable cell, the cell membrane potential and resistance characteristics were recorded in current-clamp mode (I = 0 pA).

Spontaneous IPSC (sIPSC) and EPSC (sEPSC) recordings were made in voltage clamp mode (V_m = −70 mV). Signals were stored on-line using Pulse software and were filtered at 1 kHz and digitized at 10 kHz. The liquid junction potential was approximately 9-10 mV between the pipette solution and the ACSF and was not subtracted from the data obtained.

For evoked IPSC (eIPSC) experiments, tungsten stimulating electrodes (World Precision Instruments, Sarasota, FL) were placed dorsolateral (100-200 μm distance) to the recorded cell, and stimuli were then delivered with an IsoFlex stimulus isolator (A.M.P.I., Jerusalem, Israel). For each cell, a stimulus response curve was generated, and a stimulus intensity producing a half-maximal response was used for paired-pulse experiments. Paired-pulses were delivered with a 50 ms inter-pulse interval and a 10 s interval between pairs.

Experimental Protocols

Baseline membrane potential was initially recorded for 5 min to ensure cell stability. CXCL12 (10 nM) was then added to the perfusion bath and recorded for 10 min or until a change in the resting membrane potential (drug effect) was observed. If a drug effect was present, then the cell was recorded for an additional 5 min following the stabilization of the membrane potential to its new baseline value. The drug was subsequently removed from the perfusion bath during a washout phase to determine if the cell would return to its initial baseline membrane potential. In a separate experiment, tetrodotoxin (TTX; 1 μM) pretreatment was used to test if CXCL12's membrane potential effects were direct or indirect (mediated by synaptic afferents).

All IPSC recordings were conducted in the presence of the non-*N*-methyl *D*-aspartate (NMDA) receptor antagonist 6,7-dinitroquinoxaline-2,3(1H, 4H)-dione (DNQX; 20 μM) to isolate GABA currents. For sIPSC experiments, baseline was recorded for 6 min. CXCL12 (10 nM) was then added to the perfusion bath, and sIPSC recordings were obtained for 9 min. For stimulation experiments, baseline paired-pulse data were collected for 10-20 min. CXCL12 (10 nM) was then added to the perfusion bath, and paired-pulse data was collected for an additional 10-20 min. CXCL12 effects on eIPSC recordings were also tested for CXCR4 contributions with the use of the CXCR4 receptor antagonist AMD3100 (1 μM). While AMD 3100 was initially thought to be selective for the CXCR4 receptor (Hatse et al., 2002), more recent data has shown that it may also be an allosteric agonist at the CXCR7 receptor (Kalatskaya et al., 2009). CXCR7 has been identified as a novel second target of CXCL12 (Balabanian et al., 2005; Burns et al., 2006), however, CXCR7 does not appear to be expressed in the DRN (Schonemeier et al., 2008). Therefore, we believe that the physiological effects of CXCL12 in this study and the actions of AMD3100 are likely mediated by the CXCR4 receptor. In some cells (both sIPSC and eIPSC experiments), the $GABA_A$ receptor-mediation of IPSC recordings was verified at the end of the experiment with the addition of the $GABA_A$ receptor antagonist bicuculline (20 μM). Under these conditions, bicuculline eliminated all IPSC activity (see *Figs*. 4A, 5A and 6A). Furthermore, a concentration-response analysis for CXCL12 was performed for 10 nM, 1.0 nM, and 0.1 nM concentrations using eIPSC recordings.

Glutamate mediated sEPSC recordings were isolated by addition of the $GABA_A$ receptor antagonist bicuculline (20 μM) and were recorded for 6 min. CXCL12 (10 nM) was then added to the perfusion bath, and sEPSC recordings were obtained for 9 min. In some cells, the glutamate receptor-mediation of these events was verified at the end of the experiment with

the addition of the non-NMDA glutamate receptor antagonist DNQX (20 μM). Under these conditions, DNQX eliminated all EPSC activity (data not shown).

Immunohistochemistry of the recorded cell

Following electrophysiology studies, standard immunofluorescence procedures were used to visualize the filled cell and neurotransmitter content (Beck et al., 2004). Slices were post-fixed in 4% paraformaldehyde overnight. Sections were incubated in PBS containing 0.5% Triton and bovine serum albumin for 30 min. Sections were then incubated in mouse anti-TPH antibody (1:500; Sigma-Aldrich) overnight at 4°C. Subsequently, immunohistochemical labeling was visualized using an Alexa 647-conjugated donkey anti-mouse secondary antibody (1:200; Molecular Probes) for 1 h at room temperature. Biocytin in the recorded cell was visualized using a streptavidin-conjugated Alexa 488 secondary antibody (1:200; Molecular Probes) for 1 h at room temperature.

Drugs

Most chemicals for making the ACSF and electrolyte solutions as well as bicuculline were obtained from Sigma-Aldrich. DNQX was purchased from Tocris (Ellisville, MO) and dissolved in dimethyl sulfoxide (final concentration in bath 0.015%). CXCL12 was obtained from R&D Systems (Minneapolis, MN), dissolved in dH_20 at 10 μM, and stored at 4°C for up to one week following rehydration. The CXCR4 antagonist AMD3100 was obtained from Sigma-Aldrich and dissolved in dH_20 at 1 mM and stored in 40 μl aliquots at −20°C until the day of the experiment. The final drug concentrations were: CXCL12 = 10 nM, 1 nM, and 0.1 nM; AMD3100 = 1 μM.

Data Analysis

The resting membrane potential was recorded from baseline, drug, and washout phases for each cell trace. The maximum drug baseline steady-state value was reported as the drug effect for each cell. Voltage responses to periodic intracellular current pulse injections (−300 pA) during membrane potential recordings were used to determine cell input resistance. The input resistance was calculated based on the average of three measured voltage responses taken at either the baseline or drug steady-state. Membrane potential and voltage responses to current pulses were measured using pClamp 9.0 software (Molecular Devices, Sunnyvale, CA). MiniAnalysis software (Synaptosoft, Inc., Decatur, GA) was used to analyze sIPSC and eIPSC events. For sIPSC and sEPSC recordings, noise analysis was conducted for each cell and amplitude detection thresholds set to exceed noise values. Events were automatically selected, analyzed for double peaks, and subsequently visually inspected and confirmed. Event amplitude histograms were generated and compared to the noise histogram to ensure that they did not overlap. Holding current was measured and synaptic activity analyzed for sIPSC or sEPSC frequency, amplitude, rise time (calculated from 10-90% of peak amplitude) and decay characteristics [calculated by averaging 200 randomly selected events and fitting a single (for sEPSC experiments) or double exponential function (for sIPSC experiments) from 10-90% of the decay phase]. The double exponential function for the sIPSC decay phase generated an initial fast component (fast decay) and a subsequent slow component (slow decay).

Data (sIPSCs or sEPSCs) were collected in 1 min bins during the 9 min period following drug application, taking into account a 2 min lag time from drug addition to initial drug effect due to recording chamber volume and perfusion rate. The maximum post-drug steady-state value (1 min bin) was reported as the drug effect for each cell and typically occurred 6-9 min following drug application. The frequency and amplitude of sIPSC events in individual cells were also illustrated as cumulative probability histograms for inter-event interval and amplitude. Group data were reported as mean ± SEM, with the exception of sIPSC and sEPSC rise time which was not normally distributed and was reported as median ± SEM.

eIPSC amplitude was calculated by subtracting the peak current from the current obtained during a 5 ms window immediately preceding the stimulus artifact. Baseline eIPSC amplitude was averaged from at least 60 consecutive trials calculated over at least 10 min before drug application. Paired-pulse ratio (PPR) was computed from the amplitude of the second eIPSC divided by the amplitude of the first eIPSC. CXCL12's effects were determined from an average of at least 60 consecutive trials following drug application.

Statistics

All data were first screened for normal distribution prior to selection of appropriate parametric or non-parametric tests. Statistics were analyzed using SigmaStat 3.11 software (Systat, San Jose, CA).

For immunohistochemical studies, percent colocalization of TPH-CXCL12 and TPH-CXCR4 was analyzed by two-way repeated measures ANOVA followed by post-hoc Student-Newman-Keuls tests when appropriate for pairwise comparisons. For electrophysiological studies, the effects of both CXCL12 and washout phases on the membrane potential and input resistance was analyzed by one-way repeated measures ANOVA followed by post-hoc Student-Newman-Keuls tests when appropriate for pairwise comparisons (baseline vs. CXCL12 vs. washout). Holding current or synaptic event characteristics of sIPSC and sEPSC recordings were compared between 5-HT and non-5-HT cells by unpaired Student's t-test or Mann-Whitney Rank Sum test when data were not normally distributed The impact of CXCL12 on holding current, sIPSC or sEPSC characteristics, eIPSC amplitude and PPR was analyzed by comparing pre- and post-CXCL12 values using paired Student's t-test or Wilcoxon Signed Rank Test for non-normally distributed data. For cumulative probability histograms, the control vs. drug treatments were compared by the Kolmogorov-Smirnov test (analyzed with MiniAnalysis software). Also, analysis of concentration-responses of CXCL12 on eIPSC amplitude or PPR was conducted by one-way ANOVA with post-hoc Student-Newman-Keuls tests for pairwise comparisons or Kruskal-Wallis ANOVA on Ranks with post-hoc Dunn's tests for non-normally distributed data. CXCL12 antagonist studies using AMD3100 were analyzed by one-way repeated measures ANOVA.

Results

Blocking Peptide Experiments

Fluorescent photomicrographs of CXCL12 and CXCR4 expressing DRN neurons are shown in Fig. 1H. The upper panels of CXCL12- and CXCR4-immunoreactivity in red show their extensive localization throughout the mid-DRN by confocal microscopy. The specific staining profiles for CXCL12 and CXCR4 were eliminated by preincubation of the brain section with a tenfold excess of the peptide used to generate each antibody (Fig. 1H *lower panels*).

CXCL12 and CXCR4 are expressed on TPH-positive neurons and on the same cells in the DRN

Fluorescent photomicrographs of TPH and CXCL12 or TPH and CXCR4 containing cells in the dorsomedial (DM) and ventromedial (VM) subdivisions of the DRN are shown in Fig. 1A-F. Individual panels of TPH-immunoreactivity in green and CXCL12- (*panels A-C*) or CXCR4- (*panels D-F*) immunoreactivity in red from mid-RN sections (−7.64 to −8.00 mm from bregma) indicate a high degree of colocalization of 5-HT neurons with CXCL12 or CXCR4 labeled cells in this region (Fig. 1 shows colocalization in DM-DRN (panels A, D) and VM-DRN (panel B, E); Table 2 and Fig. 2 present data from all DRN subdivisions including the LW-DRN). A limited number of 5-HT neurons not expressing CXCL12 or CXCR4 were detected as green-only labeling (Fig. 1B, D, E green arrows). Interestingly, several cell bodies with similar morphology to TPH-positive neurons were detected as single-labeled for CXCL12 or

CXCR4, suggesting that CXCL12 and CXCR4 may be present on other neurons or cells in the RN (Fig. 1B, E red arrows).

The individual images in Fig. 1C, F are representations of TPH and CXCL12 or TPH and CXCR4 localization detected in the raphe nuclei by confocal microscopy. Fig. 1C depicts a magnified image of serotonin neurons co-expressing CXCL12 (white arrows). CXCL12 appears to be distributed as discrete puncta in a cell-filled localization within the cytoplasm and processes of these neurons. In Fig. 1F, the subcellular distribution of CXCR4 is primarily localized to the outer membrane and processes of 5-HT neurons (white arrows). Also, fluorescent photomicrographs of cells labeled for CXCL12 and CXCR4 are depicted in Fig. 1G. Individual panels of CXCL12-immunoreactivity in green and CXCR4-immunoreactivity in red were captured and merged. The yellow/orange labeled cells in the merge image indicate that these neurons are double-labeled (white arrows).

Localization of CXCR4 to GABA Neurons in the Raphe Nuclei

Fluorescent photomicrographs of GAD 65/67, a marker for GABA, and CXCR4 containing cells in the DRN are shown in Fig. 1I. Individual panels of GAD 65/67-immunoreactivity in green and CXCR4-immunoreactivity in red taken in the xy-plane of RN sections indicate colocalization of CXCR4 to GABA neurons. The cell bodies and process seen in the merge image demonstrate CXCR4 localization to the soma and processes of GABA neurons in the DRN (Fig. 1I, white arrows). These data provide neuroanatomical support for CXCL12 modulation of GABA neurons, which may serve to provide local synaptic inputs to 5-HT and non-5-HT DRN neurons.

Quantification of CXCL12 and CXCR4 Colocalization to 5-HT Neurons in the Raphe Nuclei

“Total-TPH” labeled as well as TPH-CXCL12 or TPH-CXCR4 “colocalized” neurons were quantified in the DRN (DM, LW, and VM subdivisions) and MRN in four rats from sections taken at −8.00 mm from bregma (see Figure 2A) (*Methods*). Quantification data shown in Table 2 for CXCL12 and CXCR4 were consistent across the different animals as indicated by small standard error of mean values. Immunohistochemical analysis revealed a greater than 70% colocalization of CXCL12 and CXCR4 in 5-HT neurons in the RN. Fig. 2B shows that CXCL12 and CXCR4 colocalization with TPH was high in all DRN subdivisons. Two-way repeated measures ANOVA analysis indicated a significant effect of DRN subdivision ($F(2,12) = 12.5$, $p < 0.01$) but no effect of the chemokine and no interaction between the two factors. Fig. 2C shows the percent colocalization of CXCL12 and CXCR4 to 5-HT neurons in the DRN and MRN. Two-way repeated measures ANOVA analysis revealed a significant effect of raphe nucleus division ($F(1,6) = 42.15$, $p < 0.01$) and chemokine ($F(1,6) = 15.85$, $p < 0.01$) as well as a significant interaction between the two factors ($F(1,6) = 19.08$, $p < 0.01$). The percent colocalization of CXCL12 with TPH remained greater than 90% throughout the mid-level DRN and MRN. However, the percent colocalization of CXCR4 with TPH was higher in the DRN (92.5%) than in the MRN (71.7%) ($p < 0.01$) by post-hoc Student-Newman-Keuls test. In the MRN, CXCR4 also displayed a reduced colocalization with TPH as compared to CXCL12 ($p < 0.01$) (Fig. 2C).

Basal IPSC Characteristics and Holding Current

Table 3 shows baseline sIPSC characteristics from 5-HT (A) and non-5-HT DRN neurons (B) and sEPSC characteristics from 5-HT DRN neurons (C). The baseline sIPSC characteristics were not different between 5-HT and non-5-HT neurons. Furthermore, under conditions of synaptic activation no statistical difference was detected between 5-HT and non-5-HT neurons comparing baseline eIPSC amplitude and PPR characteristics (Fig. 6A’, B’ vs. Fig. 6C, C’). Holding current from all IPSC experiments was also not different between 5-HT and non-5-HT cells (5-HT: -30.8 ± 3.9 pA, $n = 28$; non-5-HT: -35.7 ± 6.4 pA, $n = 15$). These data suggest

that the resting membrane potential as well as presynaptic GABA release are similar in the two cell populations.

CXCL12's Effects on Membrane Potential and sEPSCs in 5-HT Neurons

The resting membrane potential was recorded under current clamp conditions (I = 0 pA) in 5-HT neurons located in the VM-DRN. Serotonergic neurons (n = 10) showed a statistically significant and reversible depolarization response to 10 nM CXCL12 application ($F(2,11) = 8.34$, $p < 0.01$) which averaged 7.3 ± 2.0 mV in magnitude (Fig. 3B, $p < 0.01$ when compared to baseline by post-hoc Student-Newman-Keuls test).

An example of CXCL12's depolarizing effects on 5-HT neurons is shown in the recording from a 5-HT neuron (Fig. 3A, A'), in which the cell membrane is depolarized from −61.5 mV to −53.7 mV in response to 10 nM CXCL12. The observed depolarization returned to a baseline level of −62.2 mV following drug washout. Using voltage responses to −300 pA current injections, the cellular membrane input resistance was calculated to be 300.6 MΩ at baseline and 287.1 MΩ following CXCL12 application in this serotonin cell. CXCL12 (10 nM) application produced a small (11 MΩ) but non-significant drop of input resistance from 288 ± 59 to 277 ± 54 MΩ when calculated for all recorded 5-HT neurons. Thus, CXCL12 depolarizes 5-HT DRN neurons without significantly affecting the cellular input resistance of these neurons.

TTX (1 μM) pretreatment prior to CXCL12 application blocked the depolarization effect. In the presence of TTX (n = 9), pre-CXCL12 membrane potential was −61.8 ± 2.5 and post-CXCL12 membrane potential was −61.0 ± 3.2. From these data, we can conclude that CXCL12's effect on membrane potential is indirect, mediated by synaptic afferents. In voltage clamp studies conducted in the presence of the non-NMDA glutamate antagonist DNQX (both sIPSC and eIPSC experiments), CXCL12 had no effect on holding current (pre-CXCL12 holding current: −30.8 ± 3.9 pA, post-CXCL12 holding current: −33.8 ± 5.5 pA; n = 28) in 5-HT DRN neurons. These data indicate that blockade of non-NMDA glutamate receptors prevents CXCL12's membrane effects, indicating that glutamate afferents are a likely candidate to mediate the depolarization produced by CXCL12.

To provide more direct evidence of a glutamatergic role in CXCL12's membrane effects, the action of CXCL12 on sEPSC recordings were examined. CXCL12 elevated sEPSC frequency in 5-HT DRN neurons without changing sEPSC amplitude or affecting any other sEPSC characteristics (see Table 3C). In a subset of these experiments, the glutamatergic nature of the sEPSC recordings was confirmed at the end of the experiment by total blockade of sEPSCs by DNQX (20 μM; data not shown). These experiments indicate that CXCL12 elevates presynaptic glutamate release at 5-HT DRN neurons, an effect that may underlie the membrane depolarization described above.

CXCL12's Effects on Spontaneous GABA Synaptic Currents of 5-HT and Non-5-HT Neurons

sIPSCs were recorded under voltage-clamp conditions (V_m = −70 mV) in 5-HT and non-5-HT neurons in the VM-DRN. Table 3 summarizes CXCL12's (10 nM) effects on baseline sIPSC characteristics in these two cell populations.

CXCL12's sIPSC effects on a recorded 5-HT neuron are depicted in Fig. 4A. The recorded cell was serotonergic since it was detected to be TPH positive (Fig. 4B merge, white arrow). In this cell, CXCL12 (10 nM) stimulated baseline sIPSC frequency from 8.4 Hz to 13.6 Hz and did not change sIPSC amplitude (13.7 pA to 13.6 pA). Application of bicuculline (20 μM), completely eliminated the recorded sIPSC, confirming that these events are mediated by the $GABA_A$ receptor. The increase in sIPSC frequency was statistically significant (z-score =

3.51, $p < 0.05$ by Kolmogorov-Smirnov two sample test) as indicated by a left-ward shift on the inter-event interval cumulative histogram (Fig. 4C). However, the cumulative histogram for sIPSC amplitude for baseline and CXCL12 treatment remained unchanged (Fig. 4C').

Group analysis of recorded serotonergic neurons ($n = 12$) revealed that CXCL12 significantly increased sIPSC frequency (Fig. 4D, $p < 0.01$; Table 3) with no change in sIPSC amplitude (Fig. 4D'; Table 3), indicating an enhanced presynaptic release of GABA on these neurons. CXCL12 had no effect on any other sIPSC characteristics (Table 3) or holding current analyzed in the recorded 5-HT DRN neurons (baseline holding current: −30.8 ± 3.4 pA; CXCL12 holding current: −33.8 ± 5.5 pA).

CXCL12's effects on a recorded non-5-HT neuron are depicted in Fig. 5. The recorded cell was non-5-HT since it did not label with TPH (Fig. 5B merge, white arrow). In this cell, CXCL12 (10 nM) stimulated baseline sIPSC amplitude from 25.8 pA to 33.2 pA and did not affect sIPSC frequency (10.0 Hz to 9.7 Hz). Application of bicuculline (20 μM) completely eliminated the recorded sIPSC recordings, which confirms that these events were mediated by the $GABA_A$ receptor. The increase in sIPSC amplitude was statistically significant (z-score = 3.28, $p < 0.05$ by the Kolmogorov-Smirnov two sample test) as indicated by a right-ward shift on the cumulative histogram (Fig. 5C'). However, the sIPSC inter-event interval cumulative histogram for baseline and CXCL12 treatment remained unchanged (Fig. 5C).

Unlike 5-HT neurons, non-5-HT neurons ($n = 7$) exhibited an increase in sIPSC amplitude (Fig. 5D', $p < 0.05$; Table 3) with no change in sIPSC frequency (Fig. 5D; Table 3) upon CXCL12 application. These results suggest an enhanced expression of either postsynaptic GABA receptor number or sensitivity on the recorded non-5-HT neurons. CXCL12 also did not alter any additional sIPSC characteristics (Table 3) or holding current analyzed in these cells (baseline holding current: −35.7 ± 6.4 pA; CXCL12 holding current: −33.8 ± 6.3 pA).

Thus, CXCL12 (10 nM) appears to exhibit unique actions on 5-HT vs. non-5-HT neurons in the DRN. The differences in frequency vs. amplitude recordings in these neurons indicate that CXCL12 stimulates presynaptic GABA release in 5-HT neurons and postsynaptic GABA receptor number or sensitivity in non-5-HT DRN neurons.

CXCL12's Evoked GABA Synaptic Actions on 5-HT and Non-5-HT Neurons

Additionally, we examined eIPSC recordings under voltage-clamp conditions ($V_m = -70$ mV) in 5-HT and non-5-HT neurons in the VM-DRN to complement our previous spontaneous recording data with recordings conducted under conditions of synaptic activation.

CXCL12 (10 nM) exhibited dual action on both the eIPSC amplitude and PPR in 5-HT neurons. A representative recording of a 5-HT neuron shows that CXCL12 application stimulates baseline eIPSC amplitude from 284.8 pA to 378.9 pA and reduces baseline PPR from 0.94 to 0.80 (Fig. 6A, B). The addition of bicuculline (20 μM) completely eliminated the recorded eIPSC events, thus confirming that the eIPSC recordings were mediated by the $GABA_A$ receptor (Fig. 6A).

In serotonergic neurons ($n = 15$), CXCL12 (10 nM) application significantly enhanced eIPSC amplitude (Fig. 6A', $p < 0.01$). PPR was also significantly decreased in 5-HT neurons following CXCL12 treatment (Fig. 6B', $p < 0.01$). CXCL12's ability to increase eIPSC amplitude and decrease PPR in 5-HT DRN neurons suggests that its actions are mediated by an elevated presynaptic release of GABA. These results indicate that CXCL12 enhances both spontaneous and evoked GABA release on 5-HT DRN neurons.

In contrast to CXCL12's actions in 5-HT DRN neurons, non-5-HT DRN neurons ($n = 7$) demonstrate an increase in eIPSC amplitude ($p < 0.05$) with no change in PPR following CXCL12 application (Fig. 6C, 6C'). These results suggest an enhanced GABA receptor number or sensitivity on the postsynaptic neuron mediated by CXCL12. Thus, the findings observed under conditions of evoked GABA release complement the data previously recorded under conditions of spontaneous GABA release (Fig. 5).

CXCL12's Concentration-Dependent Effect on eIPSCs

The concentration-dependent actions of CXCL12 on eIPSC GABA synaptic activity in 5-HT neurons were examined using 0.1, 1.0, and 10 nM doses of CXCL12. The 0.1 nM CXCL12 application did not change eIPSC amplitude in 5-HT DRN neurons ($n = 7$). In contrast, both 1.0 nM ($p < 0.01$, $n = 9$) and 10 nM ($p < 0.01$, $n = 14$) of CXCL12 significantly increased eIPSC amplitude above predrug baseline values. The PPR was reduced by 10 nM CXCL12 ($p < 0.01$), but not by either the 0.1 or 1.0 nM CXCL12 treatments. Fig. 7 summarizes the concentration-dependent nature of CXCL12's actions on eIPSC amplitude and PPR in 5-HT DRN neurons. There was a statistically significant drug concentration effects on eIPSC amplitude ($F(2) = 3.90$, $p < 0.05$) and PPR ($F(2) = 3.37$, $p < 0.05$) by one-way ANOVA. Post-hoc Student-Newman-Keuls tests indicated a statistically significant change in eIPSC amplitude by the 1.0 and 10 nM concentrations as compared to the 0.1 nM concentration ($p < 0.05$). The 10 nM concentration also produced a statistically significant change in PPR as compared to the 1.0 nM concentration ($p < 0.05$) but not the 0.1 nM concentration.

The CXCR4 Antagonist AMD3100 Inhibits CXCL12's Effects on GABA Synaptic Currents Evoked at 5-HT Neurons

In order to investigate if the observed effects of CXCL12 on eIPSC amplitude and PPR in 5-HT DRN neurons were mediated by the CXCR4 receptor, we utilized a CXCR4 antagonist AMD3100 prior to the application of CXCL12 (10 nM). In Fig. 8A, AMD3100 (1 μM) had no intrinsic effect on eIPSC amplitude as compared to baseline ($n = 7$). The increase in eIPSC amplitude normally produced by 10 nM CXCL12 (Fig. 6A') was absent in the presence of AMD3100 (Fig. 8A). In Fig. 8B, AMD3100 also had no intrinsic effect on PPR in 5-HT neurons, and the CXCL12 (10 nM)-induced reduction in PPR (Fig. 6B') was selectively blocked by pretreatment with AMD3100. One-way repeated measures ANOVA tests were not statistically significant for drug effects on either eIPSC amplitude or PPR in 5-HT neurons. Also, in non-5-HT neurons ($n = 8$), AMD3100 had no effect on eIPSC amplitude or PPR, and it was able to eliminate the CXCL12-mediated increase in eIPSC amplitude previously recorded in non-5-HT DRN neurons (baseline eIPSC amplitude: 343.6 ± 25.0 pA, AMD3100 eIPSC amplitude: 367.4 ± 41.0 pA, CXCL12 eIPSC amplitude: 362.7 ± 40.8 pA; baseline PPR: 0.90 ± 0.05 pA, AMD3100 PPR: 0.89 ± 0.03 pA, CXCL12 PPR: 0.90 ± 0.04 pA). One-way repeated measures ANOVA tests were also not statistically significant for drug effects on either eIPSC amplitude or PPR in non-5-HT neurons.

Discussion

In the present study, the anatomical relationship of CXCL12 and its receptor CXCR4 with 5-HT neurons in the midbrain RN as well as the functional impact of CXCL12 on 5-HT neurotransmission were investigated. Our data indicate that CXCL12 and CXCR4 constitutively colocalize with TPH in 5-HT neurons of the RN. Functionally, CXCL12 depolarizes 5-HT neurons, thus increasing their membrane excitability. This depolarization effect appears to be mediated indirectly via elevated presynaptic glutamate release. CXCL12 also stimulates presynaptic GABA release selectively at 5-HT neurons and increases postsynaptic GABA receptor sensitivity in non-5-HT neurons, both under conditions of basal and synaptically-evoked GABA release). CXCL12's GABAergic effects are concentration-

dependent and mediated by its receptor CXCR4. Its actions at 5-HT and non 5-HT DRN neurons are summarized in Table 4. These results provide important information toward understanding the neurophysiological actions of CXCL12 on the serotonin system and also support the general hypothesis that chemokines, in addition to traditional neurotransmitters and neuropeptides, provide a neuromodulatory function in the brain (Adler et al., 2005;Adler and Rogers, 2005;Rostene et al., 2007).

The advancing field of neuroimmunology has shown interest in CXCL12 and CXCR4 due to their role in neurological diseases, influence on neural development, and ability to interact with established brain systems. Immunohistochemical analysis of CXCL12 and CXCR4 labeling in the RN by confocal microscopy indicates that these immune proteins are expressed as discrete puncta in the cytoplasm and outer membrane of 5-HT cell bodies and processes. The punctate staining pattern has been observed for CXCL12 and CXCR4 in previous immunohistochemistry studies in various brain regions (Banisadr et al., 2002; Banisadr et al., 2003; Rostasy et al., 2003; Miller et al., 2005; Callewaere et al., 2008; McCandless et al., 2008) including the DRN (Banisadr et al., 2002; Banisadr et al., 2003; Callewaere et al., 2008) as well as in the periphery (Hu et al., 2007).

The subcellular localization of CXCL12 as cell-filled puncta suggests that it may be synthesized and stored in vesicles within 5-HT neurons. In previous electron microscopy studies of the rat posterior pituitary, vasopressinergic neurons were shown to contain CXCL12 in dense-core vesicles (Callewaere et al., 2008). Furthermore, although cellular processes were not stained for specific axonal or dendritic markers, the localization of CXCR4 in the outer membrane and processes of 5-HT neurons suggests that CXCL12's interactions with CXCR4 may have a role in 5-HT mediated synaptic transmission (Limatola et al., 2000). For example, CXCL12 stored within vesicles of 5-HT neurons may be co-released with or alter the release of serotonin from 5-HT neurons in the RN. A similar autocrine function has been described for CXCL12 at vasopressinergic neurons (Callewaere et al., 2006) and for other chemokines (de Jong et al., 2005). Comparable effects of colocalization and co-release have also been demonstrated for neuropeptides and neurotransmitters (Zupanc, 1996; Hokfelt et al., 2000). Therefore, CXCL12 may serve a neuromodulatory function on the serotonin system in the brain (Adler et al., 2005; Adler and Rogers, 2005; Callewaere et al., 2007).

CXCR4-immunoreactivity was also observed in non-5-HT neurons in the DRN. The double-labeling immunohistochemistry of CXCR4 and GAD 65/67 in the DRN indicates that a proportion of CXCR4-positive cells are GABAergic. These anatomical data are consistent with our electrophysiological findings that CXCL12 stimulates presynaptic GABA release at 5-HT DRN neurons. While the RN contains both GABA and glutamate neurons (Nanopoulos et al., 1982; Clements et al., 1991), both neurotransmitters have been reported to colocalize with 5-HT neurons in the RN (Belin et al., 1983; Gras et al., 2002; Fremeau, Jr. et al., 2002; Shutoh et al., 2008; Commons, 2009). Therefore, it is possible that in some cases, CXCR4 may be expressed on 5-HT DRN neurons which also colocalize with GABA or glutamate.

The quantification of immunohistochemical data presented in this report indicates a substantial degree (> 70%) of colocalization between CXCL12 and CXCR4 with TPH, the rate limiting enzyme in serotonin biosynthesis, in the mid-RN. Interestingly, TPH-CXCL12 and TPH-CXCR4 colocalization patterns are not uniform throughout the RN. On average, the DRN contains the greatest proportion of colocalized neurons (92%), with the dorsomedial subdivision revealing the greatest percent colocalization (95%), in contrast to the MRN (82%). The differential expression of these immune proteins in relation to 5-HT DRN and MRN neurons may be of functional importance since the neurons in each region have been reported to exhibit different physiological profiles and unique forebrain projections (Vertes, 1991; Vertes et al., 1999; Beck et al., 2004). This is particularly relevant for CXCR4 since our data

indicate that CXCR4 preferentially localizes to 5-HT neurons of the DRN vs. MRN. For example, greater CXCR4 localization on prefrontal cortex-projecting 5-HT neurons in the DRN may imply a particularly important role of CXCL12 in modulating higher cognitive and emotional behaviors as well as emotional dysfunction. Future studies will need to determine if the regional differences in colocalization apply to the rostro-caudal extent of the DRN as well since the anatomical and functional heterogeneity of rostral and mid vs. caudal DRN has been well documented (Abrams et al., 2004). Also, it is important to note that the inclusive term “colocalization” does not rule out the possible expression of these chemokine proteins in terminals that are synapsing onto, rather than co-expressed on 5-HT neurons. In either case, colocalization implies a chemokine interaction with the 5-HT system, but by different cellular mechanisms (i.e. co-expression of CXCL12 and 5-HT in the same neuron vs. CXCL12 containing terminals synapse on 5-HT cell bodies/processes).

To investigate the functional impact of our anatomical findings, we conducted electrophysiological studies examining the effects of CXCL12 on 5-HT neuronal properties and GABA synaptic activity. Electrophysiology studies were conduced in a somewhat broader area of the mid-level DRN (−7.56 to −8.28 mm from bregma). Our data indicate that exogenous application of CXCL12 depolarizes 5-HT neurons implying that it enhances neuronal excitability and potentially stimulates serotonin release from terminal fields. This membrane depolarization is prevented by pretreatment with TTX to block action potential-dependent synaptic neurotransmitter release, indicating an indirect effect mediated by synaptic afferents. Excitatory glutamate afferents likely mediate this depolarization because in voltage clamp experiments, CXCL12 has no significant effect on holding current when pretreated by the non-NMDA glutamate receptor antagonist DNQX. More direct evidence for this hypothesis comes from the finding that CXCL12 elevates presynaptic glutamate release at 5-HT DRN neurons. These data are also consistent with previous reports of CXCL12-induced glutamate release in other brain regions (Limatola et al., 2000; Guyon et al., 2006).

We utilized spontaneous and evoked electrophysiological techniques to investigate the indirect GABA synaptic effects of CXCL12 on 5-HT DRN neurons. Our electrophysiological results demonstrate that CXCL12 increases the frequency of sIPSC events in 5-HT neurons, yet it increases the amplitude of sIPSC events in non-5-HT neurons. Thus, CXCL12 appears to enhance both presynaptic GABA release at 5-HT neurons and postsynaptic GABA receptor number or sensitivity on non-5HT neurons. The time-course of these effects differed as would be predicted: CXCL12 effects on presynaptic GABA release peaked at 3 min in the majority of 5-HT neurons, whereas the effects on postsynaptic GABA receptors was slower, peaking at 6 min, in the majority of non 5-HT neurons.

Based on the current postsynaptic data, we cannot conclusively distinguish between increases in $GABA_A$ receptor number or sensitivity in non-5-HT cells. Future studies will be necessary to test whether the postsynaptic effect is rapidly reversible (as would be expected of a change in receptor sensitivity), or whether CXCL12 can elevate $GABA_A$ receptor number using techniques such as single cell RT-PCR. Since sIPSC experiments were conducted in the *absence* of TTX, the observed synaptic activity is responsive to both action potential-dependent and action-potential independent GABA release. Future studies examining CXCL12 effects on minature IPSC (mIPSC) recordings (in the presence of TTX) will also be necessary to determine the subcellular site of CXCL12’s actions. If CXCL12 enhances presynaptic GABA release by activating CXCR4 receptors on GABA terminals, CXCL12 should enhance mIPSC frequency. Alternatively, if CXCL12 produces its effect by activating CXCR4 receptors on GABA cell bodies or dendrites, enhancing neuronal activity and subsequently GABA release, mIPSC frequency should be unaffected by CXCL12. CXCL12’s presynaptic GABA actions have also been reported in other brain areas including the substantia nigra (Guyon et al., 2006) and lateral hypothalamus (Guyon et al., 2005a).

Additional synaptically-evoked IPSC recordings were conducted to confirm our previous electrophysiological findings under spontaneous release conditions. CXCL12 concentration-dependently increases eIPSC amplitude and decreases PPR in 5-HT neurons, whereas it only increases eIPSC without affecting PPR in non-5-HT neurons. While changes in eIPSC amplitude may be mediated by either presynaptic or postsynaptic mechanisms, changes in PPR are selectively produced presynaptically (Dobrunz and Stevens, 1997; Goda and Stevens, 1998). Thus, CXCL12's actions on GABA synaptic activity under conditions of spontaneous release are also present under conditions of synaptic activation.

CXCL12's enhancement of presynaptic GABA synaptic activity during conditions of synaptic activation was also blocked by pretreatment with the CXCR4 antagonist AMD3100, indicating that CXCL12's actions are mediated by its interactions at the CXCR4 receptor. Interestingly, AMD3100 had no intrinsic effects on GABA synaptic activity, suggesting that tonic release of CXCL12 is not observed in the slice preparation. However, a limitation of brain slice recordings is that long projection afferent fibers may be severed when slices are prepared and as a result, the tonic release of a number of neurotransmitters is absent *in vitro* when compared to conditions *in vivo*. For example, 5-HT neurons *in vivo* are spontaneously active, an effect mediated by tonic norepinephrine release (Baraban and Aghajanian, 1980; Yoshimura et al., 1985). However, in DRN brain slices, 5-HT neurons are silent because noradrenergic afferents have been cut during slice preparation (Vandermaelen and Aghajanian, 1983). As a result, future *in vivo* studies with AMD3100 will need to be conducted to determine whether CXCL12 is constitutively released within the DRN under normal and/or pathophysiological conditions.

The results suggest that CXCL12 (10 nM) depolarizes 5-HT neurons by stimulating excitatory glutamate afferents and may also potentially inhibit these neurons via inhibitory GABA synaptic inputs. Thus, CXCL12's net effects on 5-HT neurotransmission may depend upon the relative balance of these excitatory and inhibitory inputs. The concentration-effect of CXCL12 on GABA synaptic activity was determined at the 10 nM, 1.0 nM, and 0.1 nM concentrations, however, no concentration-effect curves were generated for membrane depolarization or glutamate synaptic activity. If the concentration-effect of CXCL12 is different for GABA synaptic activity vs. glutamate-mediated membrane depolarization, CXCL12 may have a net excitatory effect on 5-HT neurons at one concentration and a net inhibitory effect on 5-HT neurons at another concentration. Previous studies have shown the DRN to be under greater tonic regulation by GABA than glutamate (Tao and Auerbach, 2000; Tao and Auerbach, 2003), indicating that the inhibitory effects of CXCL12 may predominate *in vivo*. However, additional concentration-effect experiments for membrane depolarization and glutamate synaptic activty at 5-HT DRN neurons are necessary to more fully examine CXCL12's overall actions on 5-HT neurotransmission.

Recent studies in our laboratory have also examined the interactions between another chemokine, fractalkine/CX3CL1, and the 5-HT system (Kirby and Heinisch, 2008). Similar to CXCL12, CX3CL1 and its receptor CX3CR1 both showed extensive colocalization with 5-HT DRN neurons. Furthermore, electrophysiological experiments demonstrated CX3CL1 enhancement of GABA synaptic activity, though at a postsynaptic level, unlike CXCL12's presynaptic mechanism of action. Distinct from CXCL12, CX3CL1 had no effects on membrane potential in 5-HT DRN neurons. Therefore, colocalization with 5-HT neurons and enhancement of GABA synaptic activity of 5-HT DRN neurons are common features of both CXCL12 and CX3CL1.

Although studies to date have reported interactions with immune proteins and serotonin in the periphery (Watanabe et al., 2001), our results provide the first evidence of 5-HT and chemokine interactions in the brain. Our findings allow the addition of the DRN to the list of brain regions, including the hypothalamus, hippocampus, substantia nigra, and cerebellum, in which

CXCL12 exerts its central effects (Guyon et al., 2005a; Callewaere et al., 2006; Guyon et al., 2006; Skrzydelski et al., 2007; Kasiyanov et al., 2008). CXCL12's impact on 5-HT neurons in the DRN may be clinically significant since hypoactivity of the serotonin system has been linked to negative mood states (Charney, 1998).

While additional studies are necessary to investigate the overall impact of CXCL12 on 5-HT neurotransmission, a potential GABA-mediated inhibitory role of chemokines on the serotonin system may contribute to the high rate of comorbidity of immune disorders with depression (van West and Maes, 1999). Our results further indicate that chemokines may represent novel targets to treat clinical disorders with underlying 5-HT dysfunction, such as anxiety, depression, and obsessive-compulsive disorder. A better understanding of chemokine and 5-HT associations in the CNS may lead to pharmacological therapies targeting these immune proteins in the treatment of serotonin related mood disorders, including depression experienced by immune-compromised individuals.

Acknowledgments

We would like to thank Dr. Patrick Piggot, members of his laboratory, and Emily Freeman-Daniels for their technical assistance. We thank Lyngine Calizo and Sheryl Beck for assistance with the GAD immunohistochemical protocol. We also thank Dr. Mary Barbe and Dr. Martin Adler for their helpful advice and guidance in interpreting our anatomical data and examining our research report. This work was supported by an NIH grant DA 20126 given to Dr. Kirby and collaborative grants from NIH (DA 06650, M. Adler, PI) and the Pennsylvania Dept. of Health as well as an NIH Center grant (DA 13429). S. Heinisch was supported by the Pennsylvania Health Research Formula Fund.

Abbreviations

ACSF	artificial cerebrospinal fluid
CNS	central nervous system
DL	double-labeled
DM	dorsomedial
DNQX	6,7-dinitroquinoxaline-2,3(1H, 4H)-dione
DRN	dorsal raphe nucleus
eIPSC	evoked inhibitory postsynaptic current
LW	lateral wing
mIPSC	miniature spontaneous inhibitory postsynaptic current
MRN	median raphe nucleus
NMDA	non-*N*-methyl *D*-aspartate
PPR	paired-pulse ratio
RN	raphe nuclei
SDF-1α	stromal cell-derived factor-1α
sEPSC	spontaneous excitatory postsynaptic current
sIPSC	spontaneous inhibitory postsynaptic current
SL	single-labeled
TPH	tryptophan hydroxylase
TTX	tetrodotoxin
VM	ventromedial

5-HT 5-hydroxytryptamine

References

Abrams JK, Johnson PL, Hollis JH, Lowry CA. Anatomic and functional topography of the dorsal raphe nucleus. Annals of the New York Academy of Sciences 2004;1018:46–57. [PubMed: 15240351]

Adler MW, Geller EB, Chen X, Rogers TJ. Viewing chemokines as a third major system of communication in the brain. AAPS.J 2005;7:E865–E870. [PubMed: 16594639]

Adler MW, Rogers TJ. Are chemokines the third major system in the brain? J.Leukoc.Biol 2005;78:1204–1209. [PubMed: 16204637]

Bajetto A, Bonavia R, Barbero S, Florio T, Schettini G. Chemokines and their receptors in the central nervous system. Front Neuroendocrinol 2001;22:147–184. [PubMed: 11456467]

Bajetto A, Bonavia R, Barbero S, Piccioli P, Costa A, Florio T, Schettini G. Glial and neuronal cells express functional chemokine receptor CXCR4 and its natural ligand stromal cell-derived factor 1. Journal of Neurochemistry 1999;73:2348–2357. [PubMed: 10582593]

Balabanian K, Lagane B, Infantino S, Chow KY, Harriague J, Moepps B, renzana-Seisdedos F, Thelen M, Bachelerie F. The chemokine SDF-1/CXCL12 binds to and signals through the orphan receptor RDC1 in T lymphocytes. Journal of Biological Chemistry 2005;280:35760–35766. [PubMed: 16107333]

Banisadr G, Dicou E, Berbar T, Rostene W, Lombet A, Haour F. Characterization and visualization of [125I] stromal cell-derived factor-1alpha binding to CXCR4 receptors in rat brain and human neuroblastoma cells. J.Neuroimmunol 2000;110:151–160. [PubMed: 11024545]

Banisadr G, Fontanges P, Haour F, Kitabgi P, Rostene W, Melik PS. Neuroanatomical distribution of CXCR4 in adult rat brain and its localization in cholinergic and dopaminergic neurons. European Journal of Neuroscience 2002;16:1661–1671. [PubMed: 12431218]

Banisadr G, Skrzydelski D, Kitabgi P, Rostene W, Parsadaniantz SM. Highly regionalized distribution of stromal cell-derived factor-1/CXCL12 in adult rat brain: constitutive expression in cholinergic, dopaminergic and vasopressinergic neurons. European Journal of Neuroscience 2003;18:1593–1606. [PubMed: 14511338]

Baraban JM, Aghajanian GK. Suppression of firing activity of 5-HT neurons in the dorsal raphe by alpha-adrenoceptor antagonists. Neuropharmacology 1980;19:355–363. [PubMed: 6104308]

Baudouin SJ, Pujol F, Nicot A, Kitabgi P, Boudin H. Dendrite-selective redistribution of the chemokine receptor CXCR4 following agonist stimulation. Mol.Cell Neurosci 2006;33:160–169. [PubMed: 16952464]

Beck SG, Pan YZ, Akanwa AC, Kirby LG. Median and dorsal raphe neurons are not electrophysiologically identical. Journal of Neurophysiology 2004;91:994–1005. [PubMed: 14573555]

Belin MF, Nanopoulos D, Didier M, Aguera M, Steinbusch H, Verhofstad A, Maitre M, Pujol JF. Immunohistochemical evidence for the presence of gamma-aminobutyric acid and serotonin in one nerve cell. A study on the raphe nuclei of the rat using antibodies to glutamate decarboxylase and serotonin. Brain Research 1983;275:329–339. [PubMed: 6354359]

Burns JM, Summers BC, Wang Y, Melikian A, Berahovich R, Miao Z, Penfold ME, Sunshine MJ, Littman DR, Kuo CJ, Wei K, McMaster BE, Wright K, Howard MC, Schall TJ. A novel chemokine receptor for SDF-1 and I-TAC involved in cell survival, cell adhesion, and tumor development. J.Exp.Med 2006;203:2201–2213. [PubMed: 16940167]

Callewaere C, Banisadr G, Desarmenien MG, Mechighel P, Kitabgi P, Rostene WH, Melik PS. The chemokine SDF-1/CXCL12 modulates the firing pattern of vasopressin neurons and counteracts induced vasopressin release through CXCR4. Proc.Natl.Acad.Sci.U.S.A 2006;103:8221–8226. [PubMed: 16702540]

Callewaere C, Banisadr G, Rostene W, Parsadaniantz SM. Chemokines and chemokine receptors in the brain: implication in neuroendocrine regulation. J.Mol.Endocrinol 2007;38:355–363. [PubMed: 17339398]

Callewaere C, Fernette B, Raison D, Mechighel P, Burlet A, Calas A, Kitabgi P, Parsadaniantz SM, Rostene W. Cellular and subcellular evidence for neuronal interaction between the chemokine stromal cell-derived factor-1/CXCL 12 and vasopressin: regulation in the hypothalamo-neurohypophysial system of the Brattleboro rats. Endocrinology 2008;149:310–319. [PubMed: 17901225]

Charney DS. Monoamine dysfunction and the pathophysiology and treatment of depression. Journal of Clinical Psychiatry 1998;59(Suppl 14):11–14. [PubMed: 9818625]

Clements JR, Toth DD, Highfield DA, Grant SJ. Glutamate-like immunoreactivity is present within cholinergic neurons of the laterodorsal tegmental and pedunculopontine nuclei. Adv.Exp.Med.Biol 1991;295:127–142. [PubMed: 1776566]

Commons KG. Locally collateralizing glutamate neurons in the dorsal raphe nucleus responsive to substance P contain vesicular glutamate transporter 3 (VGLUT3). Journal of Chemical Neuroanatomy. 2009

Dantzer R, Kelley KW. Twenty years of research on cytokine-induced sickness behavior. Brain Behav.Immun 2007;21:153–160. [PubMed: 17088043]

de Jong EK, Dijkstra IM, Hensens M, Brouwer N, van AM, Liem RS, Boddeke HW, Biber K. Vesicle-mediated transport and release of CCL21 in endangered neurons: a possible explanation for microglia activation remote from a primary lesion. Journal of Neuroscience 2005;25:7548–7557. [PubMed: 16107642]

De Paepe B, Schroder JM, Martin JJ, Racz GZ, De Bleecker JL. Localization of the alpha-chemokine SDF-1 and its receptor CXCR4 in idiopathic inflammatory myopathies. Neuromuscul.Disord 2004;14:265–273. [PubMed: 15019705]

Dickens C, Jackson J, Tomenson B, Hay E, Creed F. Association of depression and rheumatoid arthritis. Psychosomatics 2003;44:209–215. [PubMed: 12724502]

Dobrunz LE, Stevens CF. Heterogeneity of release probability, facilitation, and depletion at central synapses. Neuron 1997;18:995–1008. [PubMed: 9208866]

Evans DL, Charney DS, Lewis L, Golden RN, Gorman JM, Krishnan KR, Nemeroff CB, Bremner JD, Carney RM, Coyne JC, Delong MR, Frasure-Smith N, Glassman AH, Gold PW, Grant I, Gwyther L, Ironson G, Johnson RL, Kanner AM, Katon WJ, Kaufmann PG, Keefe FJ, Ketter T, Laughren TP, Leserman J, Lyketsos CG, McDonald WM, McEwen BS, Miller AH, Musselman D, O'Connor C, Petitto JM, Pollock BG, Robinson RG, Roose SP, Rowland J, Sheline Y, Sheps DS, Simon G, Spiegel D, Stunkard A, Sunderland T, Tibbits P Jr. Valvo WJ. Mood disorders in the medically ill: scientific review and recommendations. Biological Psychiatry 2005;58:175–189. [PubMed: 16084838]

Fremeau RT Jr. Burman J, Qureshi T, Tran CH, Proctor J, Johnson J, Zhang H, Sulzer D, Copenhagen DR, Storm-Mathisen J, Reimer RJ, Chaudhry FA, Edwards RH. The identification of vesicular glutamate transporter 3 suggests novel modes of signaling by glutamate. Proc.Natl.Acad.Sci.U.S.A 2002;99:14488–14493. [PubMed: 12388773]

Goda Y, Stevens CF. Readily releasable pool size changes associated with long term depression. Proc.Natl.Acad.Sci.U.S.A 1998;95:1283–1288. [PubMed: 9448323]

Gras C, Herzog E, Bellenchi GC, Bernard V, Ravassard P, Pohl M, Gasnier B, Giros B, El MS. A third vesicular glutamate transporter expressed by cholinergic and serotoninergic neurons. Journal of Neuroscience 2002;22:5442–5451. [PubMed: 12097496]

Guyon A, Banisadr G, Rovere C, Cervantes A, Kitabgi P, Melik-Parsadaniantz S, Nahon JL. Complex effects of stromal cell-derived factor-1 alpha on melanin-concentrating hormone neuron excitability. European Journal of Neuroscience 2005a;21:701–710. [PubMed: 15733088]

Guyon A, Nahon JL. Multiple actions of the chemokine stromal cell-derived factor-1alpha on neuronal activity. J.Mol.Endocrinol 2007;38:365–376. [PubMed: 17339399]

Guyon A, Rovere C, Cervantes A, Allaeys I, Nahon JL. Stromal cell-derived factor-1alpha directly modulates voltage-dependent currents of the action potential in mammalian neuronal cells. Journal of Neurochemistry 2005b;93:963–973. [PubMed: 15857399]

Guyon A, Skrzydelsi D, Rovere C, Rostene W, Parsadaniantz SM, Nahon JL. Stromal cell-derived factor-1alpha modulation of the excitability of rat substantia nigra dopaminergic neurones: presynaptic mechanisms. Journal of Neurochemistry 2006;96:1540–1550. [PubMed: 16476083]

Hatse S, Princen K, Bridger G, De CE, Schols D. Chemokine receptor inhibition by AMD3100 is strictly confined to CXCR4. FEBS Letters 2002;527:255–262. [PubMed: 12220670]

Hokfelt T, Broberger C, Xu ZQ, Sergeyev V, Ubink R, Diez M. Neuropeptides--an overview. Neuropharmacology 2000;39:1337–1356. [PubMed: 10818251]

Hu X, Dai S, Wu WJ, Tan W, Zhu X, Mu J, Guo Y, Bolli R, Rokosh G. Stromal cell derived factor-1 alpha confers protection against myocardial ischemia/reperfusion injury: role of the cardiac stromal cell derived factor-1 alpha CXCR4 axis. Circulation 2007;116:654–663. [PubMed: 17646584]

Jacobs BL, Azmitia EC. Structure and function of the brain serotonin system. Physiological Reviews 1992;72:165–229. [PubMed: 1731370]

Kalatskaya I, Berchiche YA, Gravel S, Limberg BJ, Rosenbaum JS, Heveker N. AMD3100 is a CXCR7 ligand with allosteric agonist properties. Molecular Pharmacology 2009;75:1240–1247. [PubMed: 19255243]

Kasiyanov A, Fujii N, Tamamura H, Xiong H. Modulation of network-driven, GABA-mediated giant depolarizing potentials by SDF-1alpha in the developing hippocampus. Dev.Neurosci 2008;30:285–292. [PubMed: 18073458]

Kim YK, Na KS, Shin KH, Jung HY, Choi SH, Kim JB. Cytokine imbalance in the pathophysiology of major depressive disorder. Progress in Neuropsychopharmacology and Biological Psychiatry 2007;31:1044–1053.

Kirby LG, Heinisch S. Fractalkine/CX3CL1 effects on GABA synaptic activity at serotonin neurons in the rat dorsal raphe nucleus. Soc.Neurosci.Abs. 728.12. 2008 Ref Type: Abstract.

Kryczek I, Frydman N, Gaudin F, Krzysiek R, Fanchin R, Emilie D, Chouaib S, Zou W, Machelon V. The chemokine SDF-1/CXCL12 contributes to T lymphocyte recruitment in human pre-ovulatory follicles and coordinates with lymphocytes to increase granulosa cell survival and embryo quality. Am.J.Reprod.Immunol 2005;54:270–283. [PubMed: 16212649]

Limatola C, Giovannelli A, Maggi L, Ragozzino D, Castellani L, Ciotti MT, Vacca F, Mercanti D, Santoni A, Eusebi F. SDF-1alpha-mediated modulation of synaptic transmission in rat cerebellum. European Journal of Neuroscience 2000;12:2497–2504. [PubMed: 10947825]

Lu M, Grove EA, Miller RJ. Abnormal development of the hippocampal dentate gyrus in mice lacking the CXCR4 chemokine receptor. Proc.Natl.Acad.Sci.U.S.A 2002;99:7090–7095. [PubMed: 11983855]

McCandless EE, Piccio L, Woerner BM, Schmidt RE, Rubin JB, Cross AH, Klein RS. Pathological expression of CXCL12 at the blood-brain barrier correlates with severity of multiple sclerosis. Am.J.Pathol 2008;172:799–808. [PubMed: 18276777]

Meucci O, Fatatis A, Simen AA, Bushell TJ, Gray PW, Miller RJ. Chemokines regulate hippocampal neuronal signaling and gp120 neurotoxicity. Proc.Natl.Acad.Sci.U.S.A 1998;95:14500–14505. [PubMed: 9826729]

Miller JT, Bartley JH, Wimborne HJ, Walker AL, Hess DC, Hill WD, Carroll JE. The neuroblast and angioblast chemotaxic factor SDF-1 (CXCL12) expression is briefly up regulated by reactive astrocytes in brain following neonatal hypoxic-ischemic injury. BMC.Neurosci 2005;6:63. [PubMed: 16259636]

Murdoch C, Finn A. Chemokine receptors and their role in inflammation and infectious diseases. Blood 2000;95:3032–3043. [PubMed: 10807766]

Nanopoulos D, Belin MF, Maitre M, Vincendon G, Pujol JF. Immunocytochemical evidence for the existence of GABAergic neurons in the nucleus raphe dorsalis. Possible existence of neurons containing serotonin and GABA. Brain Research 1982;232:375–389. [PubMed: 7188029]

Paxinos, G.; Watson, C. The Rat Brain in Stereotaxic Coordinates. Academic Press; New York: 2005.

Pujol F, Kitabgi P, Boudin H. The chemokine SDF-1 differentially regulates axonal elongation and branching in hippocampal neurons. J.Cell Sci 2005;118:1071–1080. [PubMed: 15731012]

Ragozzino D, Renzi M, Giovannelli A, Eusebi F. Stimulation of chemokine CXC receptor 4 induces synaptic depression of evoked parallel fibers inputs onto Purkinje neurons in mouse cerebellum. J.Neuroimmunol 2002;127:30–36. [PubMed: 12044972]

Reichenberg A, Yirmiya R, Schuld A, Kraus T, Haack M, Morag A, Pollmacher T. Cytokine-associated emotional and cognitive disturbances in humans. Archives of General Psychiatry 2001;58:445–452. [PubMed: 11343523]

Rezaie P, Trillo-Pazos G, Everall IP, Male DK. Expression of beta-chemokines and chemokine receptors in human fetal astrocyte and microglial co-cultures: potential role of chemokines in the developing CNS. Glia 2002;37:64–75. [PubMed: 11746784]

Rostasy K, Egles C, Chauhan A, Kneissl M, Bahrani P, Yiannoutsos C, Hunter DD, Nath A, Hedreen JC, Navia BA. SDF-1alpha is expressed in astrocytes and neurons in the AIDS dementia complex: an in vivo and in vitro study. J.Neuropathol.Exp.Neurol 2003;62:617–626. [PubMed: 12834106]

Rostene W, Kitabgi P, Parsadaniantz SM. Chemokines: a new class of neuromodulator? Nat.Rev.Neurosci 2007;8:895–903. [PubMed: 17948033]

Schiepers OJ, Wichers MC, Maes M. Cytokines and major depression. Progress in Neuropsychopharmacology and Biological Psychiatry 2005;29:201–217.

Schonemeier B, Kolodziej A, Schulz S, Jacobs S, Hoellt V, Stumm R. Regional and cellular localization of the CXCl12/SDF-1 chemokine receptor CXCR7 in the developing and adult rat brain. J.Comp Neurol 2008;510:207–220. [PubMed: 18615560]

Shutoh F, Ina A, Yoshida S, Konno J, Hisano S. Two distinct subtypes of serotonergic fibers classified by co-expression with vesicular glutamate transporter 3 in rat forebrain. Neuroscience Letters 2008;432:132–136. [PubMed: 18222609]

Siegert RJ, Abernethy DA. Depression in multiple sclerosis: a review. J.Neurol.Neurosurg.Psychiatry 2005;76:469–475. [PubMed: 15774430]

Skrzydelski D, Guyon A, Dauge V, Rovere C, Apartis E, Kitabgi P, Nahon JL, Rostene W, Parsadaniantz SM. The chemokine stromal cell-derived factor-1/CXCL12 activates the nigrostriatal dopamine system. Journal of Neurochemistry 2007;102:1175–1183. [PubMed: 17509088]

Sozzani S, Locati M, Allavena P, Van DJ, Mantovani A. Chemokines: a superfamily of chemotactic cytokines. Int.J.Clin.Lab Res 1996;26:69–82. [PubMed: 8856360]

Stumm R, Hollt V. CXC chemokine receptor 4 regulates neuronal migration and axonal pathfinding in the developing nervous system: implications for neuronal regeneration in the adult brain. J.Mol.Endocrinol 2007;38:377–382. [PubMed: 17339400]

Stumm R, Kolodziej A, Schulz S, Kohtz JD, Hollt V. Patterns of SDF-1alpha and SDF-1gamma mRNAs, migration pathways, and phenotypes of CXCR4-expressing neurons in the developing rat telencephalon. J.Comp Neurol 2007;502:382–399. [PubMed: 17366607]

Stumm RK, Rummel J, Junker V, Culmsee C, Pfeiffer M, Krieglstein J, Hollt V, Schulz S. A dual role for the SDF-1/CXCR4 chemokine receptor system in adult brain: isoform-selective regulation of SDF-1 expression modulates CXCR4-dependent neuronal plasticity and cerebral leukocyte recruitment after focal ischemia. Journal of Neuroscience 2002;22:5865–5878. [PubMed: 12122049]

Tan Y, Shao H, Eton D, Yang Z, onso-Diaz L, Zhang H, Schulick A, Livingstone AS, Yu H. Stromal cell-derived factor-1 enhances pro-angiogenic effect of granulocyte-colony stimulating factor. Cardiovasc.Res 2007;73:823–832. [PubMed: 17258698]

Tao R, Auerbach SB. Regulation of serotonin release by GABA and excitatory amino acids. J.Psychopharmacol 2000;14:100–113. [PubMed: 10890306]

Tao R, Auerbach SB. Influence of inhibitory and excitatory inputs on serotonin efflux differs in the dorsal and median raphe nuclei. Brain Research 2003;961:109–120. [PubMed: 12535783]

Tran PB, Banisadr G, Ren D, Chenn A, Miller RJ. Chemokine receptor expression by neural progenitor cells in neurogenic regions of mouse brain. J.Comp Neurol 2007;500:1007–1033. [PubMed: 17183554]

Tran PB, Miller RJ. HIV-1, chemokines and neurogenesis. Neurotox.Res 2005;8:149–158. [PubMed: 16260392]

van West D, Maes M. Activation of the inflammatory response system: A new look at the etiopathogenesis of major depression. Neuro.Endocrinol.Lett 1999;20:11–17. [PubMed: 11473226]

Vandermaelen CP, Aghajanian GK. Electrophysiological and pharmacological characterization of serotonergic dorsal raphe neurons recorded extracellularly and intracellularly in rat brain slices. Brain Research 1983;289:109–119. [PubMed: 6140982]

Vertes RP. A PHA-L analysis of ascending projections of the dorsal raphe nucleus in the rat. Journal of Comparative Neurology 1991;313:643–668. [PubMed: 1783685]

Vertes RP, Fortin WJ, Crane AM. Projections of the median raphe nucleus in the rat. Journal of Comparative Neurology 1999;407:555–582. [PubMed: 10235645]

Watanabe T, Pakala R, Katagiri T, Benedict CR. Monocyte chemotactic protein 1 amplifies serotonin-induced vascular smooth muscle cell proliferation. J.Vasc.Res 2001;38:341–349. [PubMed: 11455205]

Yoshimura M, Higashi H, Nishi S. Noradrenaline mediates slow excitatory synaptic potentials in rat dorsal raphe neurons in vitro. Neuroscience Letters 1985;61:305–310. [PubMed: 3001598]

Zupanc GK. Peptidergic transmission: from morphological correlates to functional implications. Micron 1996;27:35–91. [PubMed: 8756315]

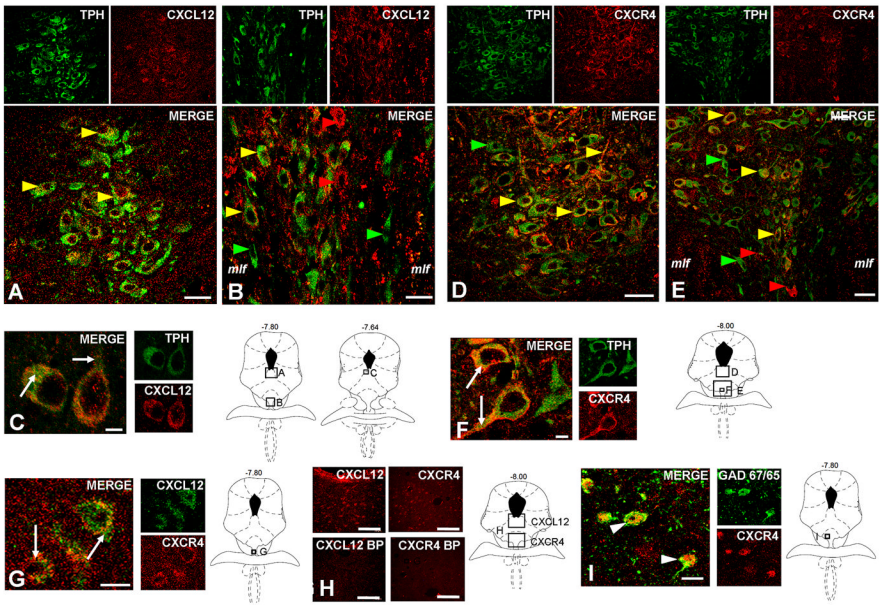

Fig. 1.

CXCL12 and CXCR4 Immunohistochemistry. Fluorescent photomicrographs of TPH with CXCL12 (A-C) or CXCR4 (D-F) containing cells in the DM (A, D) and VM (B, E) subdivisions of the DRN. The upper left panels show TPH-immunoreactivity in green, the upper right panels show either CXCL12 or CXCR4-immunoreactivity in red, and the large panels show the merge image. Colocalization of CXCL12 or CXCR4 in serotonergic neurons is present throughout the DM and VM subdivisions of the mid-DRN (yellow arrows). Individual cells were also detected to label only with TPH (green arrows), CXCL12 (red arrows; B), or CXCR4 (red arrows; E). Panels C and F show magnified fluorescent photomicrographs of CXCL12 or CXCR4 with TPH in the DRN. CXCL12 localizes as discrete puncta within the cytoplasm and processes of TPH-positive neurons, whereas CXCR4 primarily concentrates to the outer plasma membrane in TPH-positive neurons (white arrows in merge). Panel G depicts cells present within the DRN that co-express CXCL12 and CXCR4 (white arrows in merge). CXCL12 and CXCR4 antibody blocking peptide tests in the DRN were also performed (panel H). Dense DRN cellular labeling was eliminated by pre-absorption of each antibody with a 10-fold excess of the peptide used to generate the antibody (upper vs. lower images). Panel I illustrates CXCR4 expression on GABA neurons labeled with GAD-67/65 antibody in the DRN (white arrows in merge). Schematics from Paxinos and Watson (2005) are included to indicate the rostro-caudal level and localization within the DR of all immunohistochemistry panels. Scale Bars = 10 μm (C, F, G, I), 25μm (A, B, D, E) or 50 μm (H).

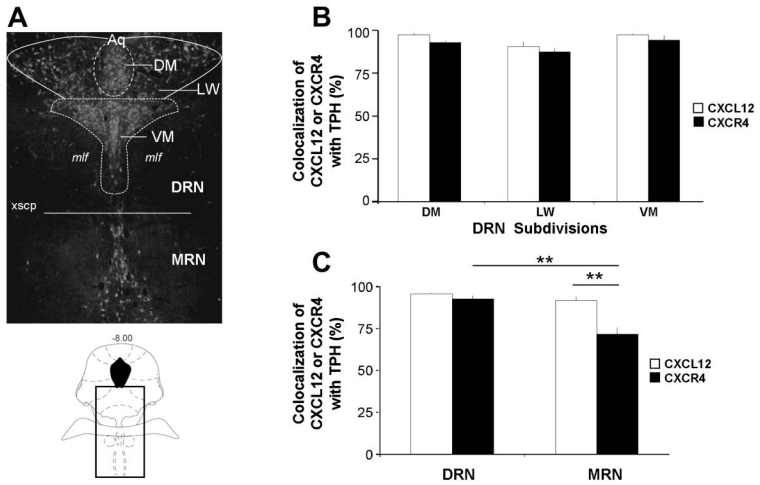

Fig. 2.

Colocalization of TPH with CXCL12 and CXCR4 in the raphe nuclei. Panel A indicates the rostrocaudal level (−8.00) (schematic in lower panel) and delineates the raphe subdivisions in which colocalization was quantified in a representative TPH-immunoreactive section of the raphe nuclei (upper panel). Panels B and C illustrate that CXCL12 and CXCR4 were found to be expressed in over 70% of serotonergic neurons throughout the subdivisions of the mid-DRN (DM, LW, VM) and MRN. Asterisks indicate significant difference by post-hoc Student-Newman-Keuls test ($p < 0.01$). All values are mean ± SEM. *DRN* = dorsal raphe nucleus; *MRN* = median raphe nucleus; *DM* = dorsomedial; *LW* = lateral wing; *VM* = ventromedial.

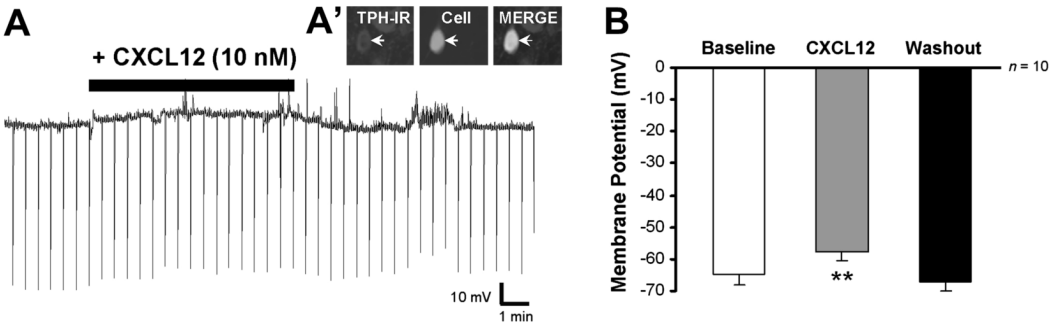

Fig. 3.

CXCL12 (10 nM) depolarizes serotonergic neurons in a reversible manner in the DRN. Resting membrane potential was recorded under current clamp conditions (I = 0 pA) in DRN neurons. Panel A' shows the immunohistochemistry of the biocytin-filled recorded neuron to be TPH-positive in the merge image (white arrow). This serotonergic neuron depolarized from −61.53 mV to −53.66 mV in response to 10 nM CXCL12 (A). Panel B represents the mean depolarization response to CXCL12 and subsequent drug washout in 5-HT DRN neurons. Serotonin neurons had an average depolarization of 7.34 ± 2.00 mV following the addition of 10 nM CXCL12. ** = $p < 0.01$ vs. baseline and washout by post-hoc Student-Newman-Keuls test. Group data are represented as mean ± SEM.

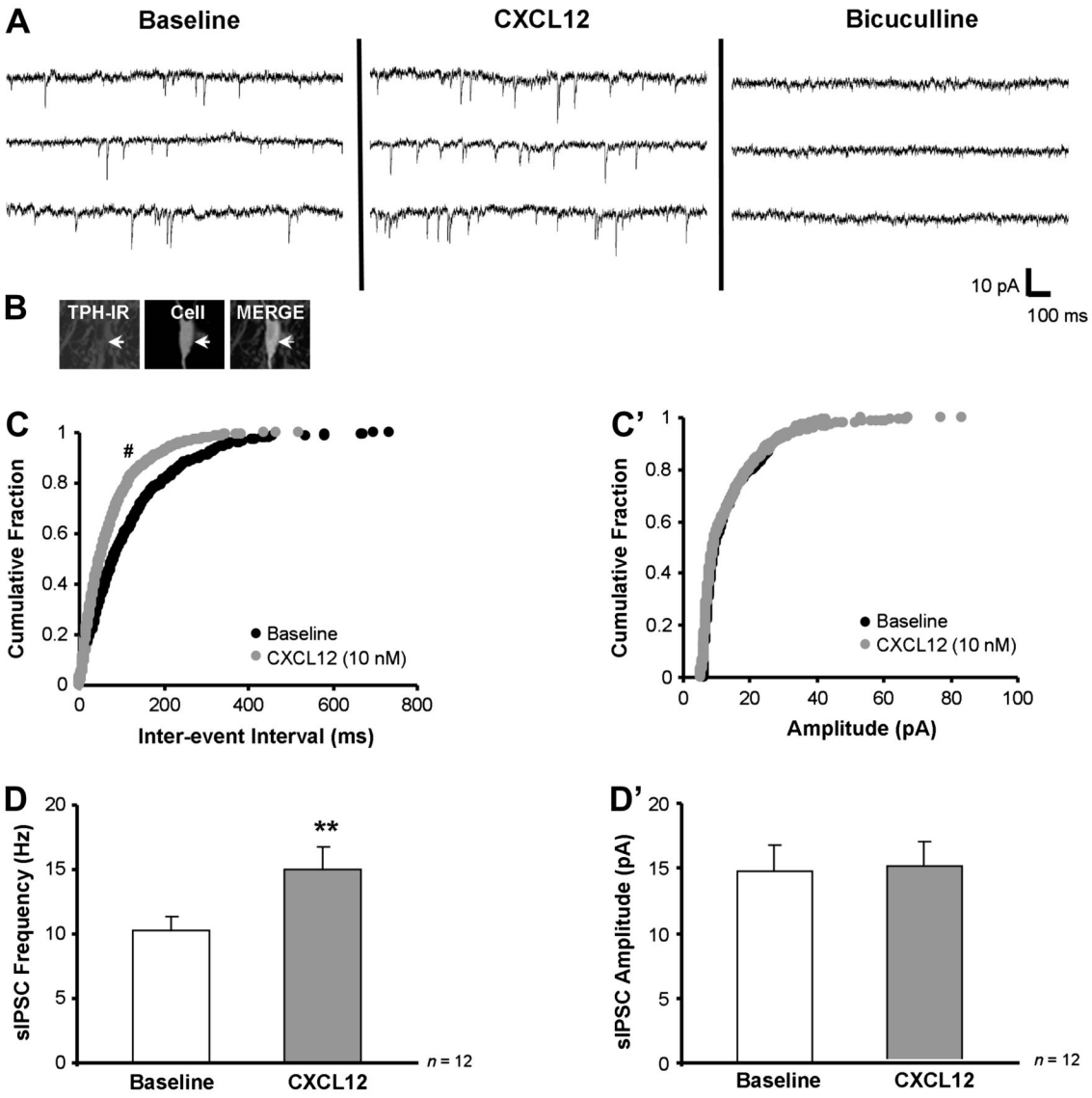

Fig. 4.

CXCL12 stimulates sIPSC frequency selectively in 5-HT DRN neurons. Panel A shows that CXCL12 (10 nM) stimulates baseline sIPSC frequency from 8.4 to 13.6 Hz without effecting sIPSC amplitude in a recorded 5-HT neuron (B, white arrow), and bicuculline (20 μM) eliminates all sIPSC events. CXCL12 produces a significant shift to the left of the cumulative histogram for inter-event interval (reflecting increased sIPSC frequency) but not amplitude (C vs. C'). Group data demonstrate that CXCL12 selectively increases sIPSC frequency (D) with no change in sIPSC amplitude (D') in 5-HT DRN neurons. ** = $p < 0.01$ by paired Student's t-test, # = $p < 0.05$ by the Kolmogorov-Smirnov two sample test. Group data are represented as mean ± SEM.

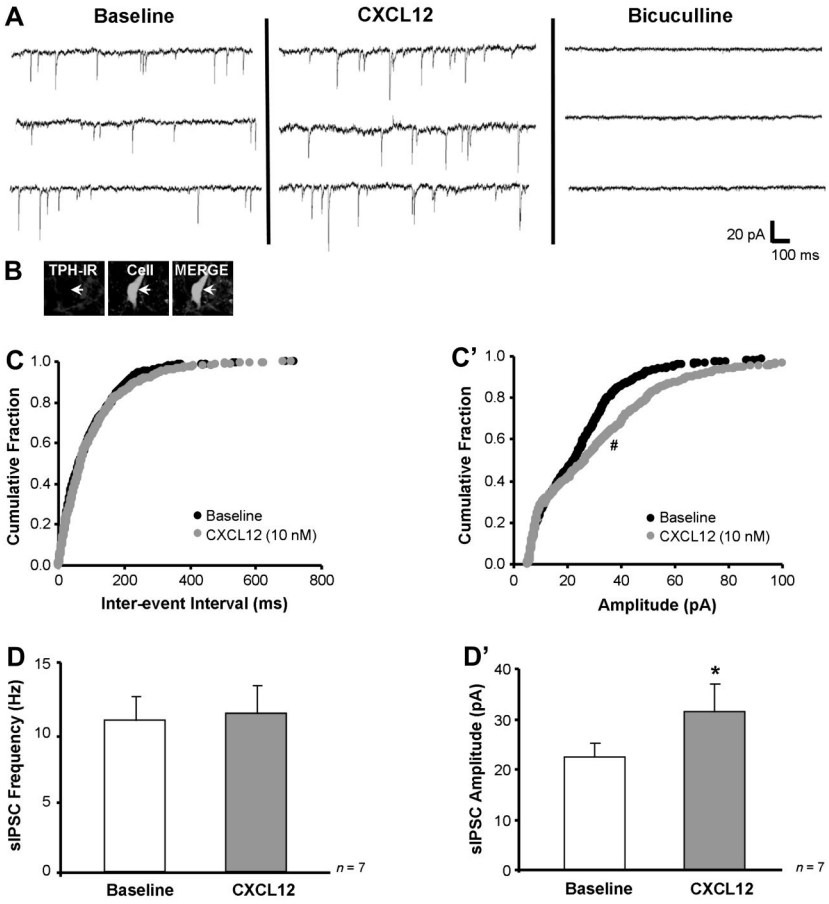

Fig. 5.

CXCL12 stimulates sIPSC amplitude selectively in non-5-HT DRN neurons. Panel A shows that CXCL12 (10 nM) stimulates baseline sIPSC amplitude from 25.8 to 33.2 pA without effecting sIPSC frequency in a recorded non-serotonergic neuron (B, white arrow), and bicuculline (20 μM) eliminates all sIPSC events. CXCL12 produces a significant shift to the right of the cumulative histogram for amplitude but not inter-event interval (C' vs. C). Group data demonstrate that CXCL12 selectively increases sIPSC amplitude (D') with no change in sIPSC frequency (D) in non-5-HT DRN neurons. * = $p < 0.05$ by paired Student's t-test, # = $p < 0.05$ by the Kolmogorov-Smirnov two sample test. Group data are represented as mean ± SEM.

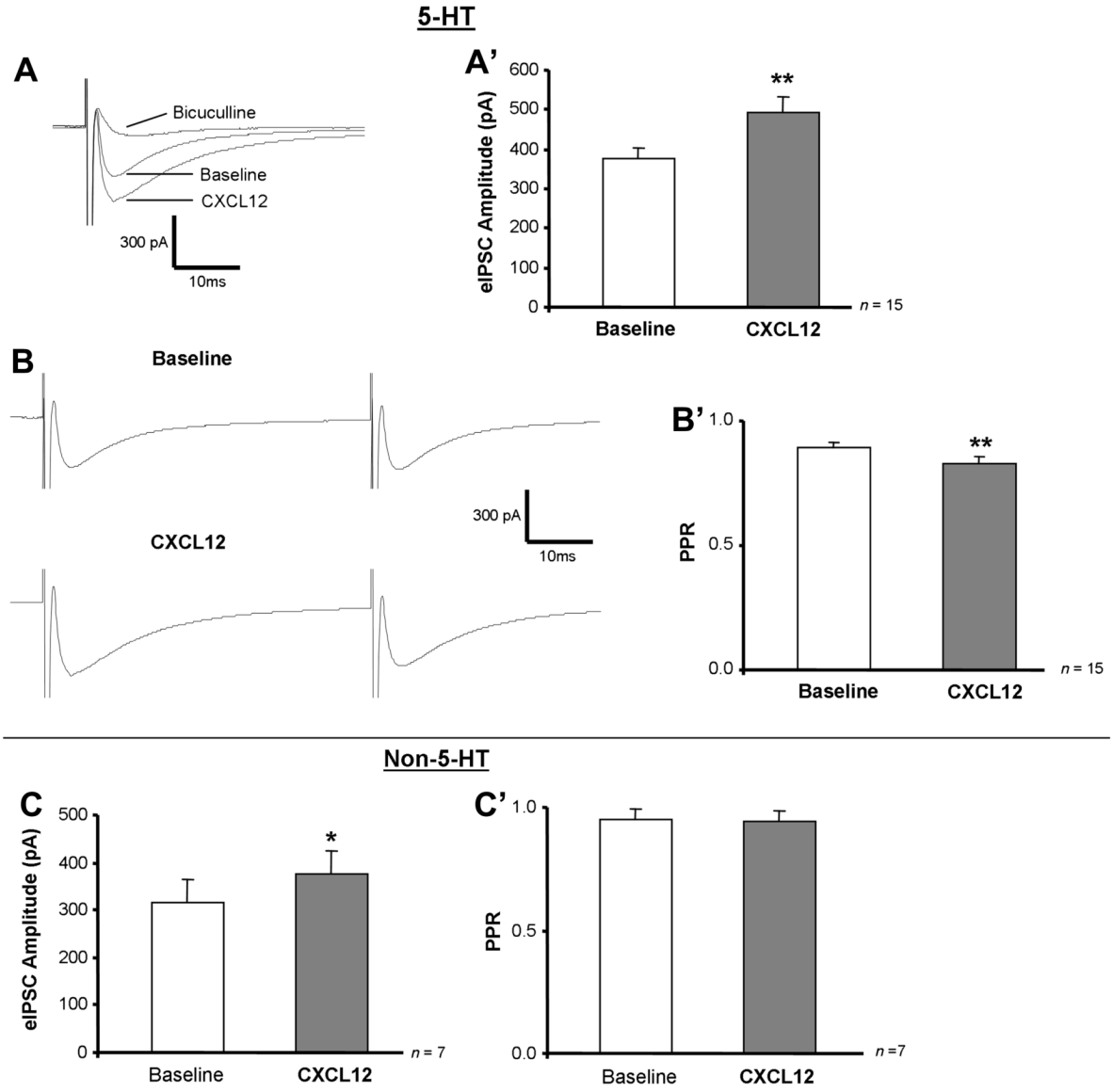

Fig. 6.

CXCL12 increases eIPSC amplitude in 5-HT and non-5-HT neurons while decreasing PPR selectively in 5-HT neurons. Panels A and B are representative traces (averaged from 60 events) showing eIPSC amplitude and PPR before and after CXCL12 and bicuculline treatment. CXCL12 (10 nM) stimulates eIPSC amplitude (A, A') and reduces baseline PPR (B, B') in 5-HT neurons, and bicuculline (20 μM) eliminates eIPSC events (A). In non-5-HT neurons, CXCL12 increases eIPSC amplitude (C) without changing PPR (C'). ** = $p < 0.01$ by paired Student's t-test (eIPSC amplitude) or Wilcoxon Signed Rank test (PPR). Group data are represented as mean ± SEM.

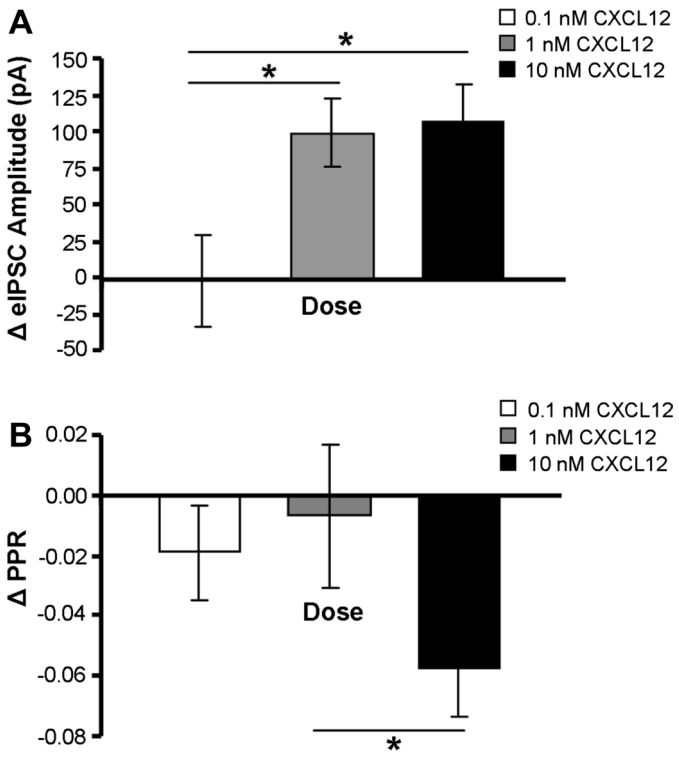

Fig. 7.

CXCL12's concentration-dependent elevation of eIPSC amplitude and depression of PPR in 5-HT DRN neurons. CXCL12 enhances eIPSC amplitude at 1.0 nM and 10 nM but not at 0.1 nM (A). CXCL12 reduces PPR at 10 nM, but not at 0.1 or 1.0 nM (B). * = $p < 0.05$ by post-hoc Student-Newman-Keuls tests. All data are represented as mean ± SEM.

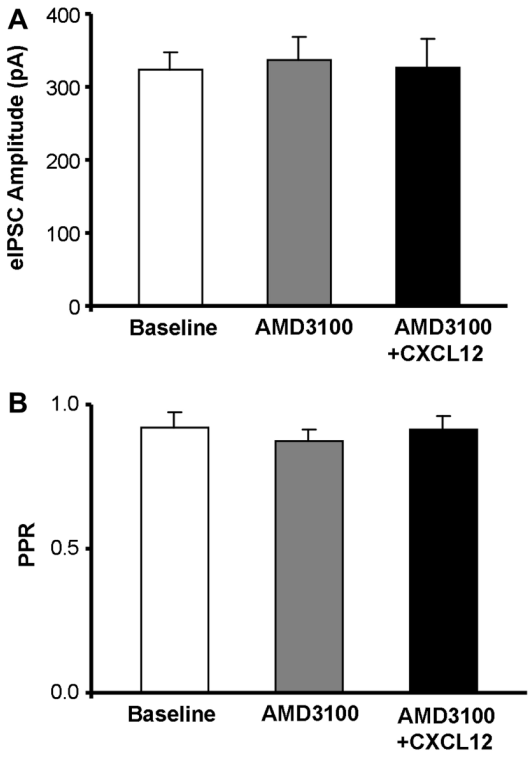

Fig. 8.

AMD3100 blocks CXCL12's effects on evoked GABA synaptic activity in 5-HT DRN neurons. AMD3100, a CXCR4 receptor antagonist, has no intrinsic effect on eIPSC amplitude (A) or PPR (B) in 5-HT neurons. The increase in eIPSC amplitude and decrease in PPR in 5-HT neurons produced by CXCL12 (see Fig. 6A'-B') was eliminated by AMD3100 (1 μM) (A, B). Statistical analysis was performed by one-way repeated-measures ANOVA. Group data are represented as mean ± SEM.

Table 1

Description of antibodies used for immunohistochemistry. SC, Santa Cruz; TP, Torrey Pines; T, Sigma; AB and MAB, Millipore.

Primary antibody	Species	Clonality	Dilution	Catalog #	Secondary antibody, Species, Dilution
Anti-CXCL12	Goat	Polyclonal	1:100	sc6193	Alexa Fluor 647. donkey anti-goat. 1:200
	Rabbit	Polyclonal	1:100	TP201	Alexa Fluor 488. donkey anti-rabbit, 1:200
Anti-CXCR4	Goat	Polyclonal	1:100	sc6190	Alexa Fluor 647, donkey anti-goat, 1:200
Anti-GAD 6&67	Rabbit	Polyclonal	1:200	AB1511	Alexa Fluor 488. donkey ant-rabbit. 1:200
Anti-NeuN	Mouse	Monoclonal	1:100	MAB377	AMCA, donkey anti-mouse, 1:100
Anti-TPH	Mouse	Monoclonal	1:500	T0678	Alexa Fluor 488, donkey anti-mouse, 1:200

Table 2

Quantification of CXCL12 and CXCR4 localized to serotonergic neurons in the mid-raphe nuclei. Colocalization quantification data of TPH with CXCL12 and TPH with CXCR4 are presented as mean number of cells ± SEM for 4 rats. *TPH* = tryptophan hydroxylase; *DRN* = dorsal raphe nucleus; *MRN* = median raphe nucleus; *DM* = dorsomedial; *LW* = lateral wing; *VM* = ventromedial; *DL* = double-labeled; *SL* = single-labeled.

Raphe nuclei subdivisions	Total TPH	TPH-CXCL12 DL	TPH SL	Total TPH	TPH-CXCR4 DL	TPH SL
DRN-DM	26.8 ± 2.7	26.0 ± 2.5	0.8 ± 0.2	29.5 ± 3.8	27.2 ± 3.2	2.2 ± 0.6
DRN-LW	32.5 ± 4.4	29.8 ± 4.9	2.8 ± 0.5	32.0 ± 1.7	28.0 ± 1.7	4.0 ± 0.7
DRN-VM	67.2 ± 3.2	65.5 ± 3.1	1.8 ± 0.2	79.5 ± 4.1	74.8 ± 3.5	4.8 ± 2.4
MRN	33.2 ± 3.3	30.5 ± 3.0	2.8 ± 0.8	22.0 ± 3.7	15.5 ± 2.2	6.5 ± 1.8

Table 3

The effect of CXCL12 on sIPSC and sEPSC characteristics in 5-HT and non-5-HT neurons. sIPSC characteristics before (baseline) and after CXCL12 (10 nM) application are presented for 5-HT (*A*) and non-5-HT (*B*) cells. sEPSC characteristics before (baseline) and after CXCL12 (10 nM) application are presented for 5-HT (*C*) cells.

Treatment	Frequency (Hz)	Amplitude (pA)	Rise 10–90% (ms)	Fast decay (ms)	Slow decay (ms)
A sIPSC characteristics in 5-HT DRN neurons					
Baseline	10.3 ± 1.1	14.8 ± 2.0	1.6 ± 0.1	3.0 ± 0.4	12.0 ± 2.0
+CXCL 12	15.0 ± 1.7**	15.2 ± 1.8	1.8 ± 0.1	4.3 ± 1.0	11.2 ± 3.0
B sIPSC characteristics in non 5-HT DRN neurons					
Baseline	11.0 ± 1.7	22.4 ± 2.9	1.5 ± 0.1	3.2 ± 0.5	17.7 ± 5.6
+CXCL 12	11.5 ± 2.0	31.5 ± 5.5*	1.4 ± 0.2	2.7 ± 0.3	13.2 ± 5.4

Treatment	Frequency (Hz)	Amplitude (pA)	Rise 10–90% (ms)	Decay (ms)
C sEPSC characteristics in 5-HT DRN neurons				
Baseline	6.1 ± 0.5	12.8 ± 0.4	1.5 ± 0.1	2.7 ± 0.1
+CXCL 12	7.5 ± 0.6*	12.2 ± 0.3	1.5 ± 0.1	2.9 ± 0.1

All values are mean ± SEM except for Rise 10-90% which is median ± SEM.

* = $p < 0.05$

** = $p < 0.01$ by paired Student's *t*-test comparing baseline vs. CXCL12 treatment groups.

Table 4

Summary of CXCL12 effects on 5-HT and non 5-HT DRN neurons.

	Membrane potential	sEPSC frequency	sEPSC amplitude	sIPSC frequency	sIPSC amplitude	eIPSC amplitude	eIPSC PPR
5-HT neurons	↑	↑	0	↑	0	↑	↓
Non 5-HT neurons				0	↑	↑	0